nature portfolio

Peer Review File

Lattice Hydrogen Transfer in Titanium Hydride Enhances Electrocatalytic Nitrate to Ammonia Conversion

Corresponding Author: Professor Weijia Zhou

Parts of this Peer Review File have been redacted as indicated to remove third-party material.

This file contains all reviewer reports in order by version, followed by all author rebuttals in order by version.

Version 0:

Reviewer comments:

Reviewer #1

(Remarks to the Author)
Li et al. reported a reversible equilibrium reaction between lattice hydrogen and activate hydrogen (H*) to improve the electrocatalytic activity of NIRR. This was an interesting work that might provide new insights into the electrochemical nitrate reduction to ammonia and the transfer of lattice hydrogen in metal hydride.
Thus, I would like to recommend it being published after some minor concerns.
(1) It was known that the maximum concentration of NO_3^- for environmental ground water should be no more than 50 ppm as required by WHO drinking water standards. It was suggested to discuss the nitrate removal rate of the catalyst after NIRR for a long time and the NO_3^- and NO_2^- contents in the final electrolyte.
(2) The process of converting NO_3^- to NH_3 involved a complex reaction requiring the transfer of 8 electrons and 9 protons, with numerous potential intermediates, so the intermediates evolution during the NIRR should be tracked by in-situ FT-IR spectra.
(3) As shown in Fig. 4h, the charge transfer kinetics of the catalyst electrode was estimated by Nyquist plots. However, the submitter did not clearly specify the conditions under which the experiment was conducted. Furthermore, the Nyquist plots should be carefully fitted with the equivalent circuit diagram and the corresponding data should be clearly listed in a table.
(4) To further demonstrated the practical applications of $TiH_{1.97}$ catalyst, the authors should continuously collect high-purity NH_3 products and characterize it.
(5) The NIRR was carried out in basic electrolyte including KOH and NO_3^- and achieved an impressive NH_3 yield rate and a high Faradaic efficiency. What about the performance in neutral electrolyte such as Na_2SO_4 with NO_3^-? The author could conduct some preliminary experiments.
(6) For DFT theoretical investigations, the authors only analyzed the NIRR activity. However, NIIR was a multi-step hydrogenation reaction, in which the formation of ammonia could be suppressed by competing reactions, especially HER. Therefore, How the catalysts suppress the competing HER should be discussed.
(7) In Fig. 5b, the author claimed that reaction energy barrier was calculated, and the climbing image nudged elastic band (CI-NEB) method was used to search for the transition states. But the calculation details (such as the images and convergence criteria) of CI-NEB were not clear, please supplement it.
(8) The stability of the NIRR catalyst required more attention. For industrial applications, stability was a very important indicator. Therefore, after the NIRR stability test, the concentration of metal ions in the electrolyte after the reaction and changed in catalyst morphology and phase should be reported.
(9) In Fig. 4a, the catalysts used for forward and reverse verification were labeled as TiH_2 and TiD_2, whereas in the article it was written as $TiH_{1.97}$. Was this labeling incorrect? This very important information should be carefully checked by the author.

Reviewer #2

(Remarks to the Author)
In this work, the authors designed and prepared $TiH_{1.97}$ by electrochemical hydrogenation reconstruction of titanium fiber paper, which achieved excellent NIRR performance. The authors emphasized that the transfer of lattice hydrogen in $TiH_{1.97}$

boosting the electrocatalytic nitrate to ammonia. These finding offered a universal design principle for metal hydride as catalysts for effectively electrochemical NH3 production, highlighting their potential for sustainable ammonia synthesis. Considering the solidness of the manuscript including synthesis, materials characterization, and electrochemical studies, I think this work can publish after the following minor revisions:
1、Why could the ECSA increase prove the adsorption of nitrate? In addition, why were the double layer capacitance negative for Ti in the electrolyte with and without NO3–. The authors should explain or provide relevant reports.
2、The authors hope to confirm the potential application of the catalyst in the field of various concentrations wastewater treatment by testing in solutions with nitrate concentrations ranging from 20 mM to 1000 mM. In fact, this concentration was too large to be applicable for currently available nitrate-rich wastewater streams like contaminated ground water (0.88-1.26 mM). The test results at lower concentrations may need to be supplemented in the paper, or the concentrated link may be included in the design of the application system to make it more complete.
3、The authors claimed that “The absorption spectrum was measured using an UV-Vis spectrophotometer and the absorption intensities at a wavelength of 220 and 275 nm were recorded. The final absorbance value was calculated by this equation: A = A220nm – 2×A275nm”. However, according to Fig. S6, the adsorption peak at 275 nm failed to be observed. Please provide a reasonable explanation.
4、To examine the local coordination environment and valence state of Ti species in TiH1.97, synchrotron-radiation-based X-ray absorption fine structure (XAFS) was utilized. However, the author did not specify the coordination number of Ti and H, so the author should make a table to include important information such as coordination number ,σ2, R factor and so on.
5、From the preparation process of TiH1.97 in experimental section, the electrolyte for electrochemical hydrogenation reconstruction was composed of 60 mmol KOH and 6 mmol KNO3 dissolved into 60 ml deionized water. Why add KNO3 to the electrolyte? Please provide a detailed explanation.
6、The colors of the TiH1.97 diagram in Fig. 2C and Fig. 4J should be unified and the author should correct it.
7、In DFT calculations, the NH3 was set as the only product through NIRR. However, due to the fact that NIRR was an 8-electron reaction, the intermediate steps were relatively complex, and there may be a large number of pathways and by-products in NIRR. Therefore, the formation of other N-containing byproducts, including NO2 and NO, should be discussed.
8、In Fig. 5c, why do proton/electron pairs prioritize attacking the N-terminal of NO? Meanwhile, has the different adsorption configurations of NO, the key intermediate of NIRR, been fully tested? Please provide a detailed explanation.

Reviewer #3

(Remarks to the Author)
The manuscript reports the use of TiH1.97 synthesized by hydrogenated reconfiguration for electrochemical nitrate reduction to ammonia. The authors claim that the TiH1.97 was successfully synthesized by electrochemical hydrogenation reconstruction of titanium fiber paper and the TiH1.97 has an impressive NH3 yield rate of 83.64 mg h–1 cm–2 and a high Faradaic efficiency (FE) of 99.11%. But a similar study has been previously reported for TiH1.97 (or TiH2), (Journal of the American Chemical Society, 2022, 144(13): 5739-5744.). The manuscript is not innovative enough, and the performance of the catalyst does not have a clear advantage over published studies at similar voltages. Therefore, I would like to recommend this manuscript to be considered by a more specific journal at this time.

A collection of (some) other issues to address is given below:

1. In Fig. 1e, the author should provide the standard spectra of Ti, TiO2 and TiH2 and should be partially zoomed in to confirm the composition of the electrodes. And if possible, it would be desirable to conduct a separate XRD test of the TiH1.97 on the electrode surface.

2. The authors should provide SEM and TEM images of the original Ti FP. And The authors should provide SEM and TEM images of the TiH1.97/Ti FP after electrocatalysis.

3. In Fig. 2d, the author should provide the standard spectrum of TiH2 (or TiH1.97). The authors should clarify whether TiH1.97 has lower or higher energy compared to Ti?

4. In Fig. S4, SAED pattern is not clear enough.

5. In Fig. 3f, when comparing the performance of nitrate reduction, authors should use comparisons under similar conditions.

6. The author first proposed the concept of lattice hydrogen in the theoretical calculation part, but it seems that there is not much connection with the experimental part. Please further explain the relationship with the experimental part in detail.

7. Incorrect captions for Fig. 3e, Fig. 3f and Fig. 3g.

8. Could the authors explain what is the proportion of Ti converted to TiH1.97 on the electrode surface? According to the XRD pattern, it seems that some Ti still exists. The authors needs more characterization to verify the composition of the electrode surface.

Reviewer #4

(Remarks to the Author)

This work demonstrated the electrochemical synthesis of titanium hydride from Ti fiber paper and reported its exceptional catalytic performance for electrochemical nitrate reduction reaction to ammonia (NIRR). The involvement of lattice hydrogen in the titanium hydride in the catalysis to provide protons to the produced ammonia was proposed and confirmed both experimentally and computationally. Other metal hybrids were also briefly tested for NIRR. Lots of experiments have been systematically conducted to make most findings and conclusions promising. The authors have done lots of work and organized the results into a well-written manuscript, and the work presented here is indeed interesting. However, the novelty of this work is not sufficient for Nature Communications. As indicated in the following specific comment (#1), the use of electrochemically synthesized titanium hydride for NIRR as well as the involvement of hydrogen from the titanium hydride during the catalysis have been already reported previously, but unfortunately, the authors did not mention this fact in the manuscript. Thus, I cannot recommend the publication of this work in Nature Communications. Since this is indeed a solid work with nice catalytic performances and experimental investigations on the proton-transfer mechanism, although its major novelty and impact were already published previously, this work may be published in a more specialized journal in the fields of fundamental catalysis or physical chemistry, after the following comments are addressed.
1. As mentioned in the general comment, the use of titanium hydride electrochemically generated from metallic Ti electrodes for NIRR was first reported by Jaramillo and coworkers in 2020 (ACS Sustainable Chem. Eng. 2020, 8, 7, 2672–2681), and Tarpeh and coworkers investigated the role of electrochemically synthesized TiHx ($0 < x \leq 2$) in NIRR in 2022 (J. Am. Chem. Soc. 2022, 144, 13, 5739–5744). The involvement of hydrogen from the titanium hydride during the NIRR, which is the main point proposed in this work, was also proposed and computationally investigated in the 2022 JACS paper. However, the authors did not mention any of them in the manuscript. The former was not even cited, and the authors only cited the latter one for indexing the crystalline lattice of TiHx without mentioning the contributions of the previous work. This is not acceptable for a work submitted to Nature Communications, as the authors were not able to justify the major novelty of their work compared to published studies.
2. The use of other metal hydrides in NIRR was also reported by others in early studies (Electrochimica Acta, 52 (2006) 1329-1338; Journal of Electroanalytical Chemistry, 599 (2007) 167-176), thus the authors should mention and cite them.
3. How did the authors determine the number "1.97" in the molecular formula? No solid proof was found in the manuscript. Without solid proof, TiHx or TiH2 may be more appropriate.
4. In addition, following the previous comment, is there any change in the ratio between titanium and hydrogen in the catalyst during the electrocatalysis? If the lattice hydrogen did involve in the electrocatalysis according to the authors' isotope experiments, the formula of the material might change.
5. The FE for ammonia reached the maxima at 50 mM of nitrate (Fig. 3c). Why?
6. The NIRR performance looks very good compared to all state-of-the-art catalysts according to Fig. 3(f). However, it should be noted that the performance was compared based on “mg/h-cm2”. Since the authors used fiber-like electrodes with a high loading of electrocatalyst and a very high ECSA, normalizing by the geometric area of electrode is not fair. The authors should quantify the loading of TiH1.97 on the surface and report the activity of their catalyst in mg/h-g or mol/h-g, then compare with other studies to see if this result really outperforms others or not.
7. Fig. S14 has a wrong caption. It should be the data for V.

Version 1:

Reviewer comments:

Reviewer #1

(Remarks to the Author)
The authors provide a suitable response and revision to my concerns. Thus, this manuscript can be accepted at its present version.

Reviewer #2

(Remarks to the Author)
The authors have positively responded all the comments raised by the reviewers. Therefore, I recommend the acceptance of this paper for publication.

Reviewer #3

(Remarks to the Author)
The authors have addressed my comments. The manuscript is now ready for acceptance.

Reviewer #4

(Remarks to the Author)
The authors have addressed all comments in a constructive way. The contributions of previous studies and the major contributors of this work compared to previous studies have been emphasized and clarified in the revised manuscript now. With these classifications, the paper can be recommended for the publication in Nature Communications. However, a few minor revisions are required prior to the acceptance of this paper.
1. In addition to the XAFS data, the PXRD data with the comparison to all standard spectra of Ti, TiH2, and TiH1.97 are also very important and informative to show that the sample here is TiH1.97. Thus, I suggest the authors to add Figure R7 in the

response to comments into the SI as well with a brief discussion in the main text.
2. The authors used XRD after electrocatalysis and XRD after isotope experiments to show that the participation of lattice hydrogen in TiH1.97 could be recovered during the NIRR process. But if we look at the XRD data in Figure S14 closely, after the NIRR at some potentials (especially at -0.8 V), the diffraction peaks of TiH1.97 become significantly weaken. Thus, it is most likely that after the reaction at a large overpotential, most lattice hydrogen atoms could not get recovered and the material started to get reduced into titanium. The authors should show the zoom-in data of Figure S14 focusing on these two diffraction peaks, and make some discussions in the revised manuscript.

Version 2:

Reviewer comments:

Reviewer #4

(Remarks to the Author)
Comments have been properly addressed with revisions made in the manuscript and SI, thus the paper can be accepted for publication.

Responses to the review's comments

We have read the referees' comments very carefully and have revised the manuscript thoroughly, considering all the feedback and suggestions. The reviewers' comments and our responses to these comments are listed below. In this response letter, the reviewers' comments are presented in black italics, our responses are in blue, and all changes are marked in red color in the revised manuscript and supporting information. We would like to thank the referees for their helpful comments and expect that we have now produced a more balanced and better account of our work. We trust that the responses and the corresponding revision of the manuscript fulfill the editor's and reviewers' requirements for considering this manuscript for publication in "***Nature Communications***". Nevertheless, if there is any further question about this submission, please feel free to let me know.

Reviewer #1 (Remarks to the Author):

Li et al. reported a reversible equilibrium reaction between lattice hydrogen and activate hydrogen (H) to improve the electrocatalytic activity of NIRR. This was an interesting work that might provide new insights into the electrochemical nitrate reduction to ammonia and the transfer of lattice hydrogen in metal hydride. Thus, I would like to recommend it being published after some minor concerns.*

(1) It was known that the maximum concentration of NO_3^- for environmental ground water should be no more than 50 ppm as required by WHO drinking water standards. It was suggested to discuss the nitrate removal rate of the catalyst after NIRR for a long time and the NO_3^- and NO_2^- contents in the final electrolyte.

Response: Many thanks for the reviewer's precious suggestion. Inspired by reviewer's precious suggestion, we provided the nitrate removal rate of the catalyst after NIRR for 3 h and the NO_3^- and NO_2^- contents in the final electrolyte. As shown in Fig. 3e, after 3 h of electrolysis, only 5.08 ppm NO_3^--N and 0.89 ppm NO_2^--N remained, both significantly below the WHO regulations for drinking water (NO_3^--N <11.3 ppm and NO_2^--N <0.91 ppm), with 98.2% NH_3 selectivity, 98.5% NO_3^- conversion.

In the revised manuscript, we have added the corresponding description as follows:

"To assess the wastewater treatment potential and ammonia production efficiency of titanium hydride. As illustrated in Fig. 3e, the NO_3^- concentration gradually decreased during NIRR −0.7 V vs. RHE. After 3 hours of electrocatalysis, only 5.08 ppm of NO_3^--N and 0.89 ppm of NO_2^--N were left, both well below the WHO standards for drinking water, indicating an NO_3^- conversion rate of 98.5% and an NH_3 selectivity of 98.2%. The 0.25 cm^2 catalyst was shown to effectively reduce NO_3^- and NO_2^- levels in 50 mL of simulated industrial wastewater to meet drinking water standards within 3 hours, showcasing its remarkable wastewater treatment capacity."

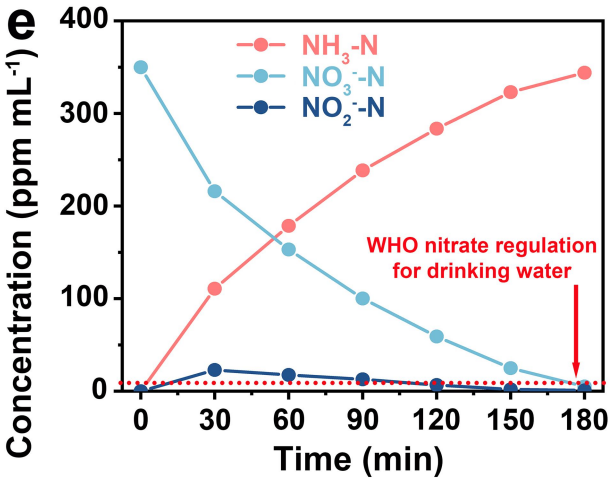

Fig. 3e Time-dependent concentration change of NO_3^--N, NO_2^--N and NH_3-N.

(2) The process of converting NO_3^- to NH_3 involved a complex reaction requiring the transfer of 8 electrons and 9 protons, with numerous potential intermediates, so the intermediates evolution during the NIRR should be tracked by in-situ FT-IR spectra.

Response: Many thanks for the reviewer's precious suggestion, which inspired us to add in-situ FTIR spectra to distinguish the reaction pathway. Herein, the in-situ ATR-FTIR spectra for titanium hydride catalyst at electrolyte with 0.1 M NO_3^- was measured from −0.1 V to −1.0 V vs. RHE to investigate the reaction process and mechanism of NIRR on the titanium hydride catalyst. The detailed description of the in-situ FT-IR spectra had been added to the revised manuscript.

In the revised manuscript, we have added the corresponding description as follows:

"We employed in-situ Attenuated Total Reflection Fourier Transform Infrared Spectroscopy (ATR-FTIR) to monitor intermediates adsorbed on the titanium hydride. As shown in Fig. S23, five distinct absorption bands were observed in the spectra of titanium hydride[15, 16]. Initially, as the potential increased, the absorption bands at 1354

cm^{-1}, corresponding to the symmetric and asymmetric N-O stretching of NO_3^-, indicated the consumption of NO_3^-. Concurrently, the downward band at 1236 cm^{-1} was attributed to the N-O antisymmetric stretching vibration of NO_2^-, signifying NO_2^- formation from the reduction of NO_3^-. With further negative shift in potential, an intermediate around 1110 cm^{-1} was attributed to the N-O stretching vibration of hydroxylamine (NH_2OH), a crucial intermediate for NH_3 formation. The presence of the characteristic peak of the -NH_2 wagging mode at 1440 cm^{-1} confirmed the formation of NH_3[17].”

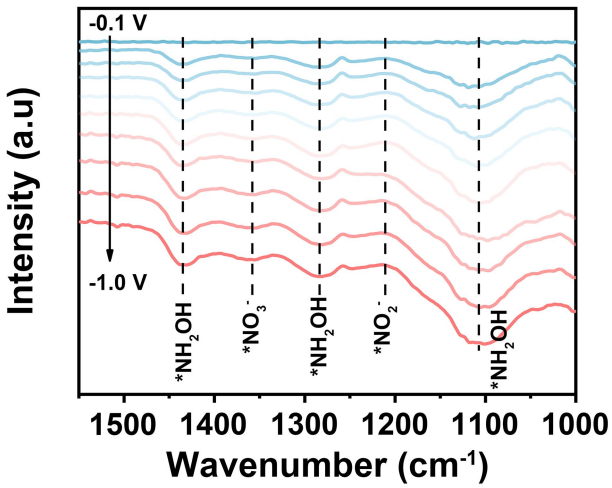

Fig. S23 In-situ ATR FTIR spectra of different intermediates in NIRR pathway.

(3) As shown in Fig. 4h, the charge transfer kinetics of the catalyst electrode was estimated by Nyquist plots. However, the submitter did not clearly specify the conditions under which the experiment was conducted. Furthermore, the Nyquist plots should be carefully fitted with the equivalent circuit diagram and the corresponding data should be clearly listed in a table.

Response: Many thanks for the reviewer’s precious suggestion. The kinetics of

charge transfer in the catalyst electrodes were evaluated using Nyquist plots under open circuit conditions (Fig. 4h). The Nyquist plots had been carefully fitted with the equivalent circuit diagram, which included substrate diffusion, potential loss and charge transfer at the electrode/electrolyte interface were labeled as R_s, R_p and R_{ct}, respectively. And the corresponding data had been clearly listed in a Table S1.

In the revised manuscript, we have added the corresponding description as follows:

"The kinetics of charge transfer in the catalyst electrodes were evaluated using Nyquist plots under open circuit conditions (Fig. 4h). These plots were meticulously fitted with an equivalent circuit diagram. The resistances corresponding to substrate diffusion, potential loss and charge transfer at the electrode/electrolyte interface were labeled as R_s, R_p and R_{ct}, respectively. The fitted data was shown in Table S1. The constant phase element (CPE) value for titanium hydride was higher than that for Ti, indicating a higher efficiency in active species adsorption for titanium hydride[39, 40]. The R_{ct} of titanium hydride was significantly lower than that of Ti FP in a 1 M KOH solution with 0.1 M NO_3^-. And, the R_{ct} of titanium hydride in 1 M KOH solution with 0.1 M NO_3^- was significantly smaller than in 1 M KOH, corresponding to faster NIRR kinetics at the titanium hydride electrode-electrolyte interface."

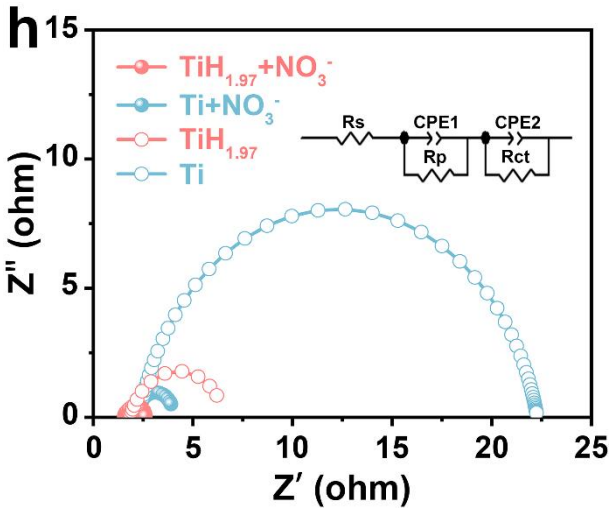

Fig. 4h The Nyquist plots.

In the revised Supporting Information, we have added the Table S1: "

Table S1. Data obtained by fitting Nyquist plots

Sample	R_s(ohm)	R_p(ohm)	CPE_1(F cm^{-2})	R_{ct}(ohm)	CPE_2(F cm^{-2})
$TiH_{1.97}+NO_3^-$	1.55	0.23	0.993	0.82	1.028
$TiH_{1.97}$	1.803	0.07	1.115	4.751	0.865
$Ti+NO_3^-$	1.998	0.252	1.084	1.759	1.047
Ti	2.13	0.174	1.047	19.97	0.823

(4) To further demonstrated the practical applications of $TiH_{1.97}$ catalyst, the authors should continuously collect high-purity NH_3 products and characterize it.

Response: We are deeply grateful for the reviewer's invaluable suggestions. Motivated by these insights, we collected high-purity NH_3 products after 24 hours of prolonged electrocatalysis and conducted characterization. In the process of treating simulated industrial wastewater, air stripping was effectively employed to extract ammonia (NH_3), resulting in a valuable end product. According to the previous

literature *(Nat. Commun 15, 2816, (2024))*, approximately 98% of NH_3 could be efficiently removed from the treated wastewater under operational conditions of 70 ℃ and an air flow, without affecting other impurities. Following NH_3 extraction, HCl was used to capture the ammonia, producing ammonium chloride (NH_4Cl). Subsequently, a rotary evaporator was used to separate NH_4Cl. Additionally, direct infusion of NH_3 into water resulted in ammonia monohydrate ($NH_3 \cdot H_2O$). XRD and ^1H NMR analyses were performed to confirm the purity of the resultant products. As shown in Fig. R1a and R1b, these analytical techniques verified that the high-purity NH_4Cl(s) and $NH_3 \cdot H_2O$(aq) obtained from the treated industrial wastewater were free of noticeable impurities. In conclusion, the employed air stripping method was an effective and selective strategy for extracting NH_3 from simulated industrial wastewater, yielding high-purity valuable products such as NH_4Cl and $NH_3 \cdot H_2O$.

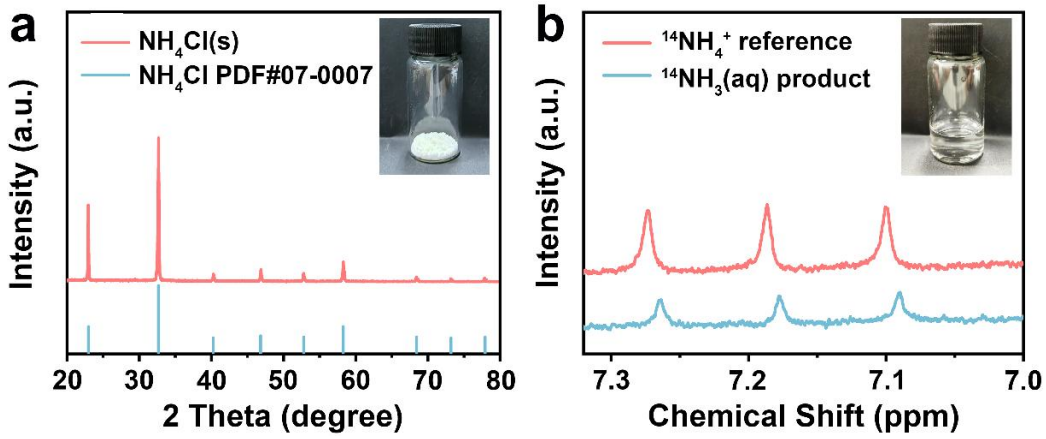

Fig. R1 (a) Synthesized NH_4Cl(s) products and its XRD analysis result. **(b)** ^1H NMR analysis of the synthesized NH_3(aq). Inset: the products itself.

(5) The NIRR was carried out in basic electrolyte including KOH and NO_3^- and achieved an impressive NH_3 yield rate and a high Faradaic efficiency. What about the performance in neutral electrolyte such as Na_2SO_4 with NO_3^-? The author could conduct some preliminary experiments.

Response: Many thanks for the reviewer's precious suggestion. Inspired by reviewer's precious suggestion, we added the NIRR performance of titanium hydride in 0.5 M Na_2SO_4 and 0.1 M NO_3^- (pH=7) in Fig. R2, the current density of $TiH_{1.97}$ significantly increased after adding NO_3^- to the electrolyte (Fig. R2a), confirming that $TiH_{1.97}$ could effectively reduce NO_3^-. The corresponding current density of titanium hydride reached up to 0.2 A cm^{-2} at −0.6 V vs. RHE. At the same potential, the maximum FE of 98.5% with an NH_3 yield of 12.75 mg h^{-1} cm^{-2} was achieved (Fig. R2b). Through this preliminary experiment, we found that this catalyst also had a good NIRR performance in a neutral electrolyte.

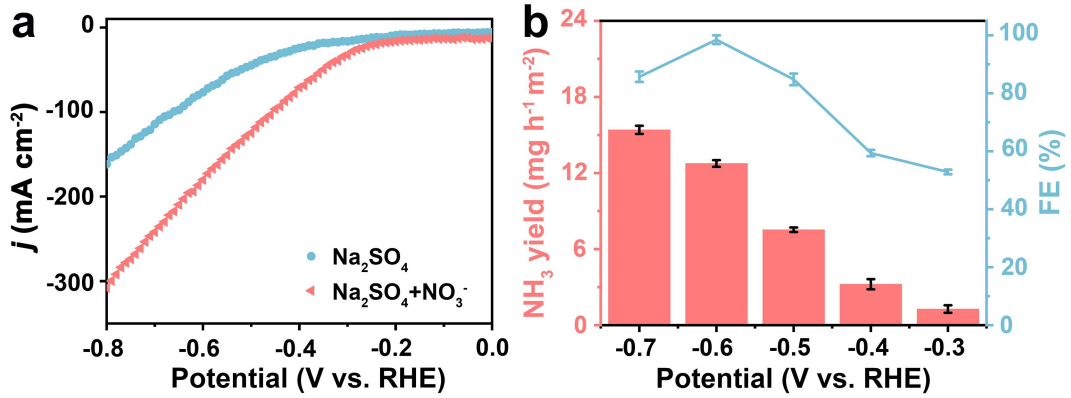

Fig. R2 (a) LSV curves, **(b)** NH_3 yield rate and FE for titanium hydride against various work potentials in 0.5 M Na_2SO_4 and 0.1 M NO_3^-.

(6) For DFT theoretical investigations, the authors only analyzed the NIRR activity. However, NIIR was a multi-step hydrogenation reaction, in which the formation of ammonia could be suppressed by competing reactions, especially HER. Therefore, How the catalysts suppress the competing HER should be discussed.

Response: Thanks for your valuable comments, which is helpful to improve this work. According to your suggestion, the reaction free energy of HER on Ti (−1.20 eV), $TiH_{1.97}$ (H-determined 0.63 eV), $TiH_{1.97}$ (Ti-determined −0.98 eV) and $TiH_{1.97}$ with H vacancy (−1.64 eV) were calculated, as shown in Fig. R3. It could be found that the limiting potentials of HER on $TiH_{1.97}$ and $TiH_{1.97}$ with H vacancy were 0.63 and −1.64 eV, respectively. By comparison, the limiting potentials of NIRR on $TiH_{1.97}$ was only 0.12 V (Fig. 5c), indicating that the HER was suppressed effectively.

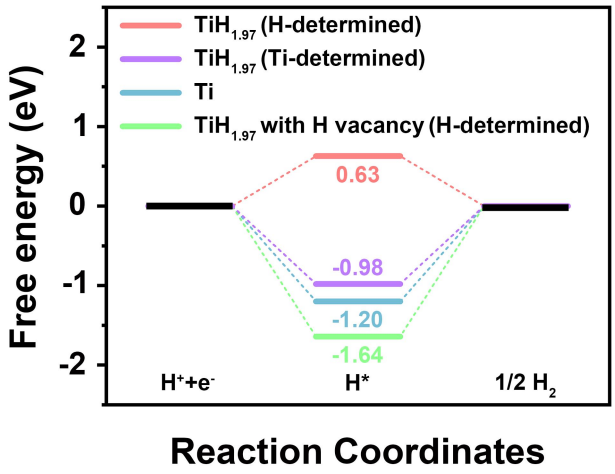

Fig. R3 Calculated reaction free energy of HER.

(7) In Fig. 5b, the author claimed that reaction energy barrier was calculated, and the climbing image nudged elastic band (CI-NEB) method was used to search for the transition states. But the calculation details (such as the images and convergence

criteria) of CI-NEB were not clear, please supplement it.

Response: Many thanks for the reviewer's precious suggestion. We were very sorry for this carelessness, the relevant details had been supplemented in section of calculation details. To calculate the kinetic energy barrier of chemical reactions, the climbing image nudged elastic band (CI-NEB) method with 6 images was used to search for the transition states (vibrational frequencies were evaluated to confirm minima and transition states), in which all of the force components erpendicular to the tangent of the reaction path were relaxed to be less than 0.05 eV/Å. This detail has been described in detail in Section 1.7. Computational details in the Supplementary Information.

(8) The stability of the NIRR catalyst required more attention. For industrial applications, stability was a very important indicator. Therefore, after the NIRR stability test, the concentration of metal ions in the electrolyte after the reaction and changed in catalyst morphology and phase should be reported.

Response: Thanks to the comments. According to the reviewer's suggestions, we have detected the concentration of Ti ions in the electrolyte after the catalysis. Through the ICP test, we could see that the Ti ion concentration in the electrolyte was only 0.07 ug/mL, there was almost no titanium ion dissolution from the electrodes. In addition, we had also added SEM image and XRD patterns after stability testing, and found that the morphology and structure of $TiH_{1.97}$ had not undergone significant changes. These results fully demonstrate the stability of the $TiH_{1.97}$ electrode.

In the revised manuscript, we have added the corresponding description as follows:

"After long-time cyclic testing, we had thoroughly characterized the titanium hydride catalyst. The SEM and XRD analyses of the titanium hydride showed that the morphology and phase of the material had not changed (Fig. S12, Fig. S13). The above results further confirmed the stability of titanium hydride during the NIRR process."

In the revised Supporting Information, we have added: "

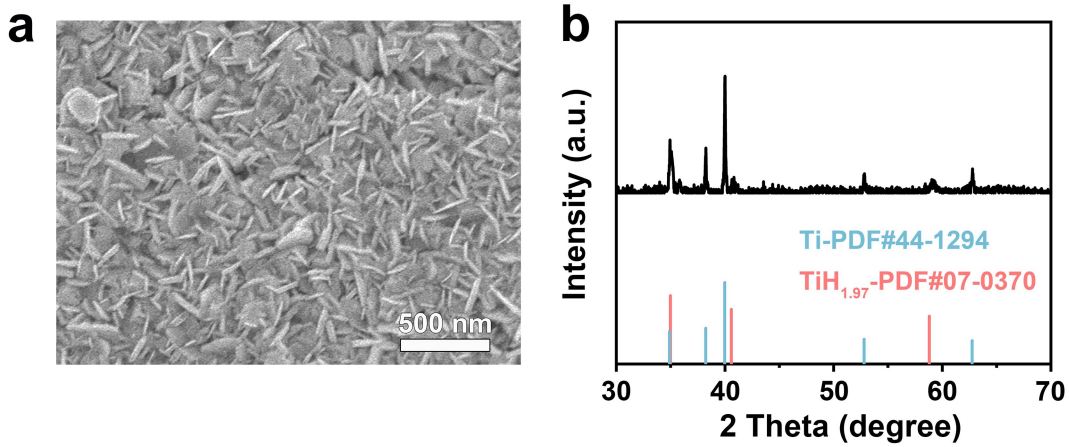

Fig. S12 (a) SEM image and **(b)** XRD patterns of titanium hydride after stability testing."

(9) In Fig. 4a, the catalysts used for forward and reverse verification were labeled as TiH_2 and TiD_2, whereas in the article it was written as $TiH_{1.97}$. Was this labeling incorrect? This very important information should be carefully checked by the author.

Response: We would thank for the reviewer's valuable comments and suggestions. According to the reviewer's suggestion, we carefully checked and revised the "TiH_2 and TiD_2" to "$TiH_{1.97}$ and $TiD_{1.97}$" in the Fig.4a.

In the revised manuscript, we have modified **Fig. 4a:**

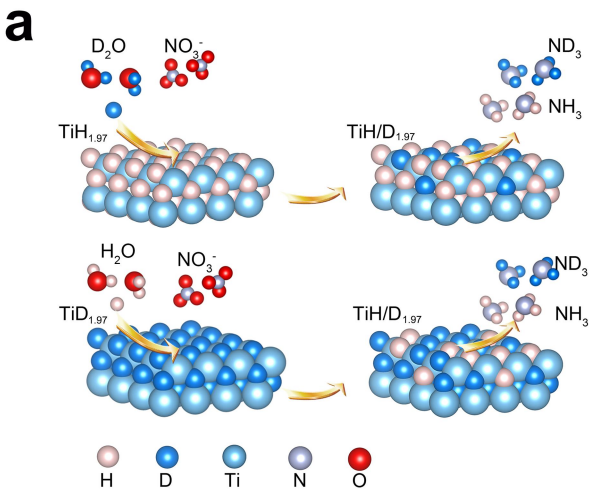

Fig. 4 (a) Model diagrams for positive and reverse validation of isotope labeled lattice hydrogen transfer in NIRR process.

Reviewer #2 (Remarks to the Author):

In this work, the authors designed and prepared $TiH_{1.97}$ by electrochemical hydrogenation reconstruction of titanium fiber paper, which achieved excellent NIRR performance. The authors emphasized that the transfer of lattice hydrogen in $TiH_{1.97}$ boosting the electrocatalytic nitrate to ammonia. These finding offered a universal design principle for metal hydride as catalysts for effectively electrochemical NH_3 production, highlighting their potential for sustainable ammonia synthesis. Considering the solidness of the manuscript including synthesis, materials characterization, and electrochemical studies, I think this work can publish after the following minor revisions:

1. *Why could the ECSA increase prove the adsorption of nitrate? In addition, why were the double layer capacitance negative for Ti in the electrolyte with and without NO_3^-. The authors should explain or provide relevant reports.*

Response: Thanks to the comments.

(1) The ECSA increase proved the adsorption of nitrate which was shown in the latest literature (*Energy Environ. Sci., 2023,16, 663-672*). The authors claimed that "In 1 M KOH without NO_3^-, the $Ni_3Fe–CO_3$ LDH/Cu foam electrode showed 2.29 mF cm^{-2} of C_{dl} which was 2.77 times higher than that of the Cu foam electrode. This indicated that both H_2O and OH^- could be adsorbed actively on $Ni_3Fe–CO_3$ LDH rather than on a Cu surface. Whereas in 1 M KOH with 0.05 M KNO_3, the C_{dl} of the Cu foam electrode increased 2.45 times implying that most NO_3^- adsorbs on the Cu surface because the C_{dl} of the $Ni_3Fe–CO_3$ LDH with or without NO_3^- is the same."

(2) In order to confirm from the actual test that the increase of ECSA means the adsorption of nitrate, the adsorption capacity test of titanium hydride and titanium was evaluated as shown in Fig. R4. The catalysts titanium hydride and titanium for NO_3^-, the catalyst with an area of 0.5*0.5 cm^2 was immersed in 5 mL, 6.2 mg L^{-1} NO_3^- solution. After conducting 200 cycles of CV testing in the no-Faradaic range, the NO_3^- content in the electrolyte was detected. As shown in Fig. R4, after the absorption by titanium hydride and titanium, the concentration of the NO_3^- solution with an initial concentration of 6.21 mg L^{-1} decreases to 6.19 mg L^{-1} and 5.75 mg L^{-1}. The absorption capacities of Ti FP and titanium hydride for NO_3^- are 0.04 μg cm^{-2} and 1.80 μg cm^{-2}, respectively. The change trend of ECSA was consistent with the calculated absorption capacities of catalysts. This indicated that the greater increase of ECSA means the stronger absorption capacity for NO_3^-.

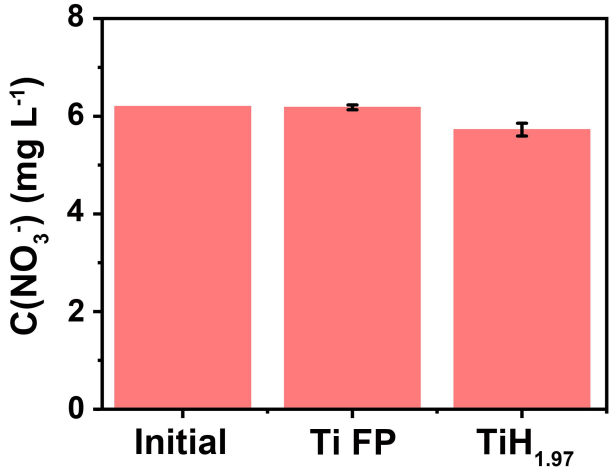

Fig. R4 The concentration of nitrate in the electrolyte after the adsorption by titanium and titanium hydride.

(3) The reason why the difference in C_{dl} of titanium with and without the addition of NO_3^- was a negative value mainly due to follow:

During the nitrate reduction process, for the titanium electrode, in the electrolyte environment without NO_3^-, the OH^- in the solution was more easily adsorbed on the catalytic active sites of titanium and was reduced to H_2O. However, when NO_3^- was added to the electrolyte, the adsorption capacity of the Ti electrode for NO_3^- was relatively weak, but the concentration of OH^- would also be reduced, resulting in a decrease in the catalytic active sites *(Energy Environ. Sci., 2023, 16, 2991; Energy Environ. Sci., 2023, 16, 663)*. Therefore, the change in ion concentration after the addition of nitrate would affect the structure of the electric double layer, reducing the electric double layer capacitance.

2. The authors hope to confirm the potential application of the catalyst in the field of various concentrations wastewater treatment by testing in solutions with nitrate concentrations ranging from 20 mM to 1000 mM. In fact, this concentration was too large to be applicable for currently available nitrate-rich wastewater streams like contaminated ground water (0.88-1.26 mM). The test results at lower concentrations may need to be supplemented in the paper, or the concentrated link may be included in the design of the application system to make it more complete.

Response: Thank you for the reviewer's suggestion. According to the reviewer's suggestions, we tested the NIRR performance under extremely low nitrate concentrations (1 M KOH +0.001 M NO_3^-), as shown in Fig. R5.

(1) The NIRR performance of titanium hydride in 1 M KOH +0.001 M NO_3^- was added in Fig. R5. When NO_3^- was added to the electrolyte, the current density of titanium hydride was slightly increased, which was mainly due to the low concentration of NO_3^-. And a 17.65% NH_3 FE with the NH_3 yield rate of 1.30 mg h^{-1} cm^{-2} was achieved at −0.4 V vs. RHE.

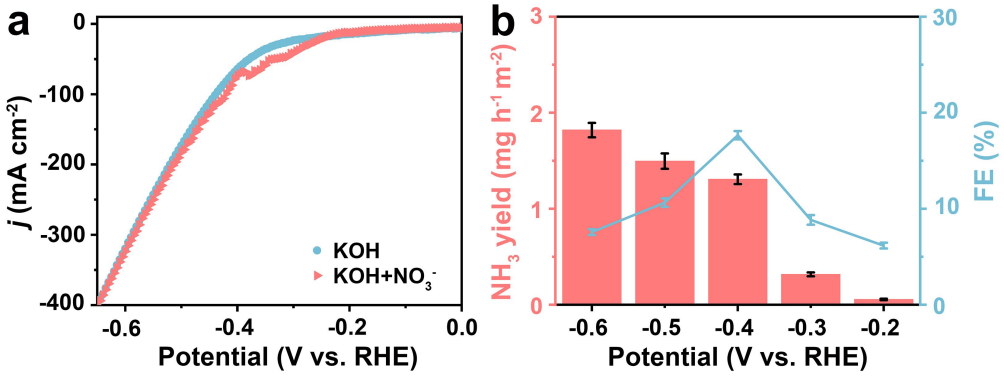

Fig. R5 (a) LSV curves, **(b)** NH_3 yields and FEs for titanium hydride against various work potentials in 1 M KOH and 0.001 M NO_3^-.

(2) The reasons why we chose to test in an electrolyte with concentration of NO_3^- (0.1 M) were as follows. Firstly, in the actual treatment of nitrate wastewater, it was easier and cheaper to use biological methods to treat low concentration nitrate wastewater, and this technology had been developed very mature. However, high concentration nitrate wastewater, such as nitrate concentration solution and landfill leachate, could not be treated by biological methods, due to the high concentration of nitrate makes it difficult for microorganisms to survive. Electrochemical nitrate reduction was a relatively effective and promising method. Secondly, from the perspective of synthetic ammonia, a high concentration of nitrate solution made it easy to achieve efficient and high-yield synthetic ammonia.

3. The authors claimed that "The absorption spectrum was measured using an UV-Vis spectrophotometer and the absorption intensities at a wavelength of 220 and 275 nm were recorded. The final absorbance value was calculated by this equation: A = A220nm – 2×A275nm". However, according to Fig. S6, the adsorption peak at 275 nm failed to be observed. Please provide a reasonable explanation.

Response: Thanks to the comments. The method (Environmental Protection Industry Standard of the People's Republic of China, Water quality–Determination of nitrate-nitrogen–Ultraviolet spectrophotometry, HJ/T 346–2007) provided in this paper was often used in the actual wastewater test. Some dissolved organic substances in the actual wastewater would have absorption peaks at 220 nm and 275 nm at the same time, while nitrate had no absorption peak at 275 nm. Therefore, by deducting the absorption peak at 275 nm, nitrate concentration could be effectively corrected to obtain a more realistic value. Because, the electrolyte used in our experiment only contains potassium nitrate and potassium hydroxide, so there was no absorption peak at 275 nm. In summary, in our testing system, the absorbance at 220 nm could be directly detected without considering the absorption peak at 275 nm. Therefore, we had made modifications to the testing method.

In the revised Supporting Information, we modified:

"**(2) Determination of nitrate-N**

Firstly, a certain amount of electrolyte was taken out from the electrolytic cell and diluted to 5 mL to detection range. Then, 0.1 mL 1 M HCl and 0.01 mL 0.8 wt% sulfamic acid solution were added into the aforementioned solution. The absorption

spectrum was measured using an UV-Vis spectrophotometer and the absorption intensities at a wavelength of 220 were recorded. The final absorbance value was calculated by this equation: $A = A_{220\ nm}$. The concentration-absorbance curve was calibrated using a series of standard potassium nitrate solutions and the potassium nitrate crystal was dried at 105-110 ºC for 2 h in advance."

4. *To examine the local coordination environment and valence state of Ti species in* $TiH_{1.97}$*, synchrotron-radiation-based X-ray absorption fine structure (XAFS) was utilized. However, the author did not specify the coordination number of Ti and H, so the author should make a table to include important information such as coordination number, σ2, R factor and so on.*

Response: Thanks to the comments. Inspired by reviewer's precious suggestion, we added the detail information in Table S2.

In the revised Supporting Information, we added the Table S2 as follow:

Table S2. Structural parameters of Ti, $TiH_{1.97}$ and TiH_2 extracted from the EXAFS fitting.

Sample	Scattering path	CN	R(Å)	σ^2/ Å^2	R factor
$TiH_{1.97}$	Ti-Ti1.1	12	3.13	0.006	0.011
TiH_2	Ti-Ti1.1	12	3.14	0.004	0.005
Ti fiol	Ti-Ti1.1	6	2.90	0.012	0.013

The S_0^2 was fixed as 0.7. The interatomic distances (R) and coordination numbers (CN). The CN was the coordination number; R was the half path length of the path,

for a single scattering path, it was the inter-atomic distance. σ^2 was the mean square variation in path length, this parameter encapsulates both static and thermal disorder. ΔE_0 was an adjustment to the E_0 used to evaluate the wavenumber of the theory, it is useful to think of ΔE as the parameter which aligns the energy grids of the data and the theory. R factor was used to indicate the accuracy of the fitting. The fitted ranges for k and R spaces were selected to be k=3-12.4 $Å^{-1}$ with R=1.5-3.5 Å (k^3-weighted).

5. *From the preparation process of $TiH_{1.97}$ in experimental section, the electrolyte for electrochemical hydrogenation reconstruction was composed of 60 mmol KOH and 6 mmol KNO_3 dissolved into 60 ml deionized water. Why add KNO_3 to the electrolyte? Please provide a detailed explanation.*

Response: Thank you for the valuable comments from the reviewers. In order to explain the role of KNO_3 in the electrochemical reconstruction process of Ti FP, we performed electrochemical reconstruction on Ti FP in electrolytes with (1#) and without (2#) the addition of KNO_3 and tested its NIRR performance. It could be seen from the XRD pattern (Fig. R6a) that the electrodes formed by the electrochemical reconstruction of Ti FP were composed of Ti (PDF#44-1294) and $TiH_{1.97}$ (PDF#07-0370) in the electrolyte with and without KNO_3, indicating that adding KNO_3 did not affect the phase structure of catalyst. In addition, the samples obtained under two conditions were tested for NIRR performance, and it could be seen from LSV curves that they had the same NIRR performance (Fig. R6b), which indicated that adding KNO_3 had no effect on NIRR performance. Therefore, it could be concluded from the above results that adding KNO_3 or not in the electrolyte had no effect on the experimental results.

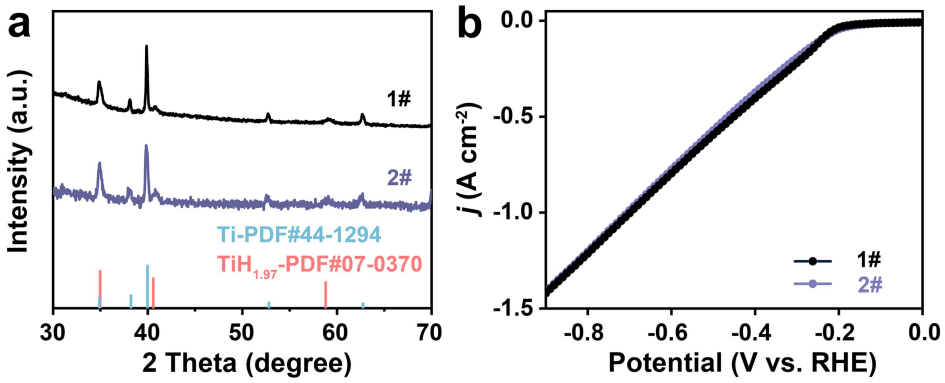

Fig. R6 (a) XRD spectrum and **(b)** LSV curve for electrochemical reconstruction of Ti fiber paper in solutions with (1#) and without (2#) the addition of KNO_3.

6. The colors of the $TiH_{1.97}$ diagram in Fig. 2C and Fig. 4J should be unified and the author should correct it.

Response: Thank you for the reviewer's suggestion. We have checked thoroughly and unified the color of the schematic diagrams of the titanium hydride structure in Fig. 2c and Fig. 4j in the revised manuscript.

In the revised manuscript, we have modified Fig. 2c: "

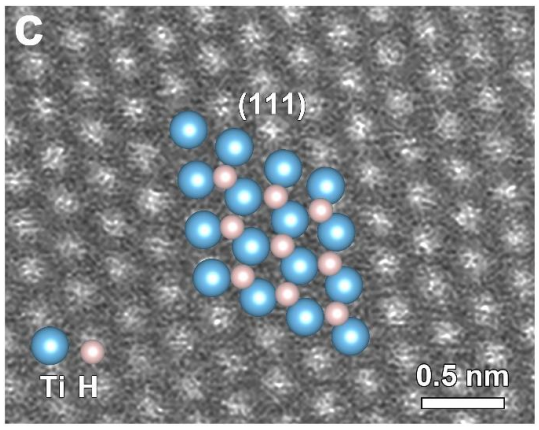

Fig. 2 (c) Atomic-resolution HAADF-STEM image of titanium hydride."

7. In DFT calculations, the NH_3 was set as the only product through NIRR. However, due to the fact that NIRR was an 8-electron reaction, the intermediate steps were relatively complex, and there may be a large number of pathways and by-products in NIRR. Therefore, the formation of other N-containing byproducts, including NO_2 and NO, should be discussed.

Response: Thank you for the reviewer's suggestion.

(1) In DFT calculations: According to the reviewers' suggestions, the formation of NO_2 and NO on $TiH_{1.97}$ were further calculated. The reaction free energy of potential determining step on $TiH_{1.97}$ was 0.12 eV, while the calculated desorption energy barriers for the release of $*NO_2$ and *NO on $TiH_{1.97}$ are 1.21 and 1.26 eV, respectively, indicating the considerably difficult formation of NO_2 and NO.

(2) In the experiment: we added in-situ FTIR spectra to distinguish the reaction pathway and intermediates. Herein, the in-situ ATR-FTIR spectra for titanium hydride catalyst at electrolyte with 0.1 M NO_3^- was measured from −0.1 V to −1.0 V vs. RHE to investigate the reaction process and mechanism of NIRR on the titanium hydride catalyst. The detailed description of the in-situ FT-IR spectra had been added to the Supporting information.

In the revised Supporting information, we added the corresponding description as follows**:**

"We employed in-situ Attenuated Total Reflection Fourier Transform Infrared Spectroscopy (ATR-FTIR) to monitor intermediates adsorbed on the titanium hydride. As shown in Fig. S23, five distinct absorption bands were observed in the spectra of

titanium hydride[15, 16]. Initially, as the potential increased, the absorption bands at 1354 cm^{-1}, corresponding to the symmetric and asymmetric N-O stretching of NO_3^-, indicated the consumption of NO_3^-. Concurrently, the downward band at 1236 cm^{-1} was attributed to the N-O antisymmetric stretching vibration of NO_2^-, signifying NO_2^- formation from the reduction of NO_3^-. With further negative shift in potential, an intermediate around 1110 cm^{-1} was attributed to the N-O stretching vibration of hydroxylamine (NH_2OH), a crucial intermediate for NH_3 formation. The presence of the characteristic peak of the -NH_2 wagging mode at 1440 cm^{-1} confirmed the formation of NH_3[17].”

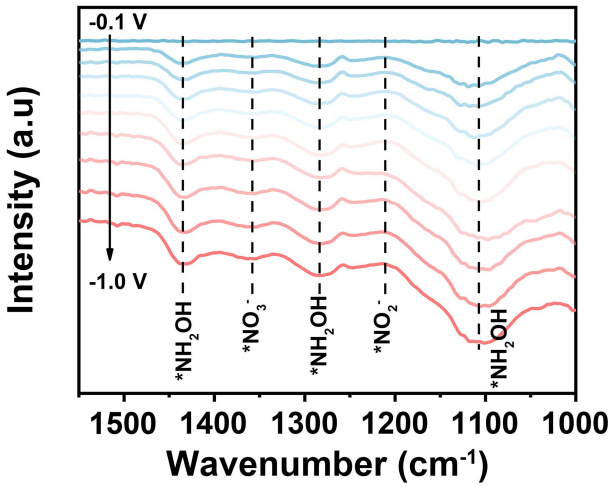

Fig. S23 In-situ ATR FTIR spectra of different intermediates in NIRR pathway.

8. In Fig. 5c, why do proton/electron pairs prioritize attacking the N-terminal of NO? Meanwhile, has the different adsorption configurations of NO, the key intermediate of NIRR, been fully tested? Please provide a detailed explanation.

Response: Thank you for the reviewer’s suggestion. According to the reviewers’ suggestions, we calculated the reaction free energy from *NO to *NOH by different

terminal atom.

In the revised Supporting Information, we added the corresponding description as follows:

"As shown in Fig. S30, it could be found that the reaction free energy from *NO to *NO-H (0.22 eV) was higher than that from *NO to *H-NO (−0.38 eV), indicating the priority of N-terminal of NO during hydrogenation process. In addition, the different adsorption configurations of NO on $TiH_{1.97}$ were tested, as shown in Fig. S31. By comparing the adsorption free energy of NO, we could conclude that NO tends to adsorb on $TiH_{1.97}$ in a lying mode with ΔG (*NO) of −1.26 eV."

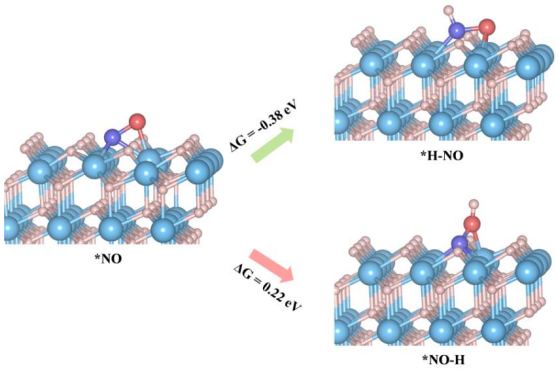

Fig. S30 Calculated reaction free energy from *NO to *NO-H and *H-NO.

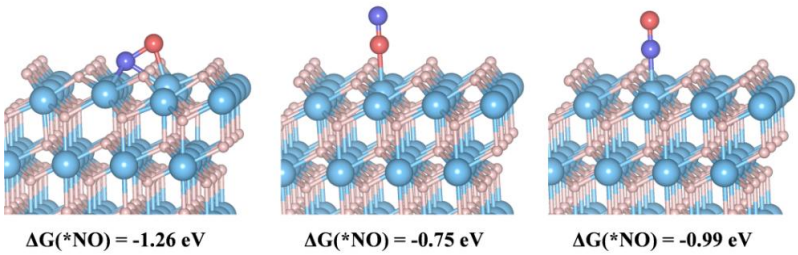

Fig. S31 Different adsorption configurations and corresponding adsorption free energies of NO on $TiH_{1.97}$.

Reviewer #3 (Remarks to the Author):

The manuscript reports the use of $TiH_{1.97}$ synthesized by hydrogenated reconfiguration for electrochemical nitrate reduction to ammonia. The authors claim that the $TiH_{1.97}$ was successfully synthesized by electrochemical hydrogenation reconstruction of titanium fiber paper and the $TiH_{1.97}$ has an impressive NH_3 yield rate of 83.64 mg h^{-1} cm^{-2} and a high Faradaic efficiency (FE) of 99.11%. But a similar study has been previously reported for $TiH_{1.97}$ (or TiH_2), (Journal of the American Chemical Society, 2022, 144(13): 5739-5744.). The manuscript is not innovative enough, and the performance of the catalyst does not have a clear advantage over published studies at similar voltages. Therefore, I would like to recommend this manuscript to be considered by a more specific journal at this time.

Response: Thank you for providing the detailed feedback on the manuscript. Your assessment and recommendations are very thoughtful and will be valuable for the authors to consider.

(1) We have carefully read the literature. In which, a research group from Stanford University led by William A. Tarpeh reported that the NIRR on titanium exhibited significant surface reconstruction and formed titanium hydrides (TiHx, 0<x<2) (Journal of the American Chemical Society, 2022, 144(13): 5739-5744.). They used ex-situ GIXRD and XAS demonstrated that the near-surface TiH_2 phase became more enriched as the applied potential and duration of the NIRR increase. This work emphasized the importance of relating NIRR performance to the near-surface electrode structure to advance catalyst design and operation. **High-activity TiH_x**

catalysts had been reported, but the catalytic mechanism was still based on the traditional proton-transfer mechanism that the H* was derived from the electrolyte not the lattice hydrogen transfer mechanism. The structure-activity relationship of TiH_x catalysts had been discussed, but the mechanism of lattice hydrogen participation in the hydrogenation process had not been fully clarified.

(2) In our manuscript, the synthesis of titanium hydride and its high catalytic activity were not the main innovations. Our primary innovation lied in the participation of lattice hydrogen in the hydrogenation reaction of NIRR, this viewpoint differed from the traditional proton transfer mechanism that the H* originates from the electrolyte, which had not been explored in previous studies. We had proved the rationality of our proposed viewpoint through isotope tracking experiments and theoretical calculation results as follow:

① To reveal the reaction mechanism for enhancing NIRR catalytic activity, isotope tracking experiments were used to investigate the electrochemical behavior of lattice hydrogen transfer from titanium hydride. The model diagram for the positive and reverse verification of isotope-labeled lattice hydrogen transfer during the NIRR process was shown in Fig. 4a. For the positive verification, titanium hydride and titanium hydride serving as electrocatalysts and using 1 M NaOD + 0.1 M KNO_3 in D_2O solution as the electrolyte for NIRR, the peaks at 7.05, 7.14 and 7.23 ppm in the ^1H NMR spectrum of Ti were identified as the characteristic peaks of ND_4^+. In the ^1H NMR spectrum of $TiH_{1.97}$, besides the characteristic peaks of ND_4^+, a set of typical peaks for NH_4^+ at 7.03, 7.12, and 7.20 ppm was observed, which were attributed to

the lattice hydrogen in titanium hydride (Fig. 4b). In the reverse verification, using the same method, we synthesized the $TiD_{1.97}$ catalyst (The XRD and solid-state NMR spectra used to confirm the successful synthesis of $TiD_{1.97}$ were shown in Fig. S18) and used 1 M NaOH + 0.1 M KNO_3 in H_2O solution as the electrolyte for NIRR. In the ^1H NMR spectrum of $TiD_{1.97}$, in addition to the characteristic peaks of NH_4^+, the typical peaks of ND_4^+ were also noted, indicating their origin from lattice deuterium in $TiD_{1.97}$ (Fig. 4c). Through the aforementioned positive and reverse verification, we had concluded that the lattice hydrogen in $TiH_{1.97}$ indeed participated in the hydrogenation reaction of NIRR. Lattice hydrogen effused from titanium hydride and was converted into H*, while the H* in the solution ensured the formation of titanium hydride. The reversible equilibrium reaction between lattice hydrogen and H* not only enhanced the electrocatalytic activity of NIRR but also exhibited excellent catalytic stability.

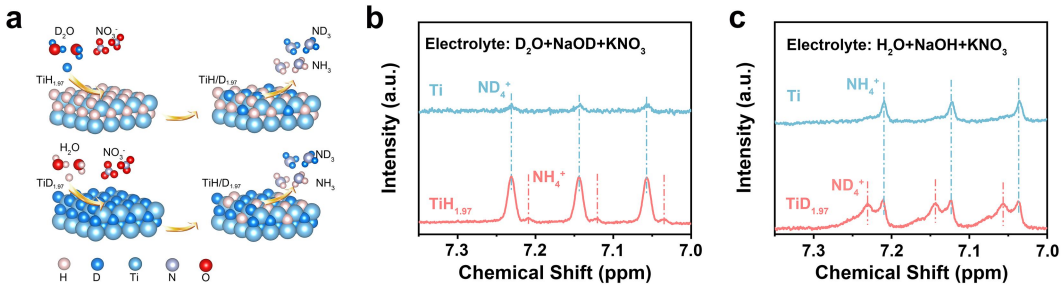

Fig. 4 (a) Model diagrams for positive and reverse validation of Isotope labeled lattice hydrogen transfer in NIRR process. **(b)** Isotope labeled lattice hydrogen transfer in NIRR process for $TiH_{1.97}$ (positive validation) and **(c)** $TiD_{1.97}$ (reverse validation).

The detail isotope tracking experiments had been written in Supporting Information as follows:

1.3 Isotope labeled active hydrogen transfer in NIRR.

Positive validation method for the participation of lattice hydrogen in hydrogenation reactions in titanium hydride. In an H-type electrolysis cell, a $TiH_{1.97}$/Ti catalyst was prepared. A D_2O solution containing 1 M NaOD and 0.1 M KNO_3 was used as the electrolyte for NIRR. Both the Ti FP and the synthesized $TiH_{1.97}$/Ti electrode were rinsed with D_2O for 10 minutes and dried at 250 ℃ under argon for 24 h to remove H_2O. NIRR was conducted at −0.7 V vs. RHE for 5 min, after which 10 mL of electrolyte was taken out and adjusted to pH = 4 with 2 M D_2SO_4, and the resulting products, NH_3 and ND_3, were explored using ^1H NMR.

Reverse validation method for the participation of lattice hydrogen in hydrogenation reactions in titanium hydride. In an H-type electrolysis cell, a $TiD_{1.97}$/Ti catalyst was prepared by cathodic electrochemical reconstruction for 30 min in a D_2O + NaOD + NO_3^- solution. Subsequently, an H_2O solution containing 1 M NaOH and 0.1 M KNO_3 was used as the electrolyte for NIRR. NIRR was conducted at −0.7 V vs. RHE for 5 min, after which 10 mL of electrolyte was taken out and adjusted to pH = 4 with 2 M D_2SO_4, and the resulting products, NH_3 and ND_3, were explored using ^1H NMR.

In order to more intuitively understand the process of isotope tracking experiment, we have added the flow chart in Supporting information as below:

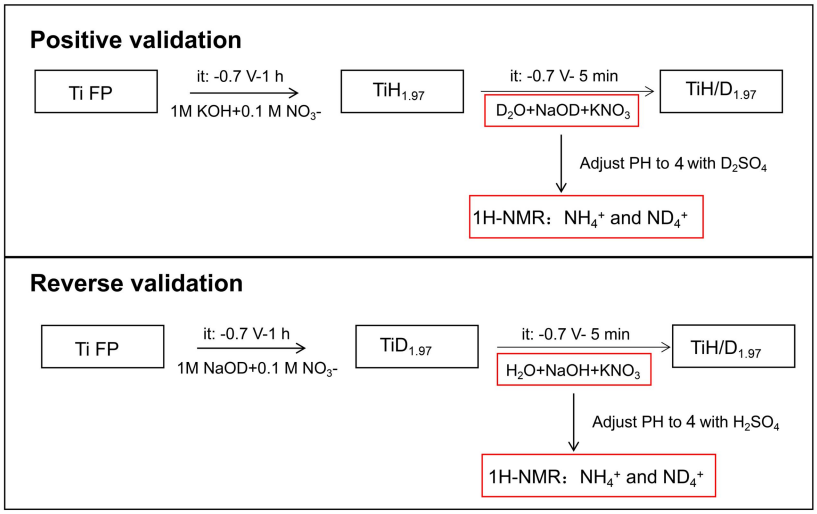

② As for density functional theory calculations, we lied emphasis on the competitive behavior between different sources of H* during the hydrogenation process of NIRR (one was from electrolyte, the other was from the lattice hydrogen in $TiH_{1.97}$). By calculating the reaction energy barriers, we found that the lattice H* would preferentially participate in the NIRR rather than the H* from the H_2O solution. More importantly, it could be found that the spillover and supplementation of lattice H could balancing the adsorption strength of key reaction intermediates, subsequently, the NIRR was effectively promoted.

(3) More importantly, the proposed mechanism of lattice hydrogen participating in catalytic reversible reactions could be extended to other metal hydrides, such as **palladium hydride (Fig. S24), tantalum hydride (Fig. S25), and vanadium hydride (Fig. S26)**. Additionally, this mechanism of lattice hydrogen facilitating catalytic reactions might also have implications for other hydrogenation reactions, such as the hydrogenation of CO_2.

(4) To clarify the mechanism of hydrogenation reactions involving lattice hydrogen, we had reorganized the development process of titanium hydride electrocatalysts in the introduction.

In the revised manuscript, we have reorganized the introduction content as follows:

"In order to rationally design NIRR catalysts, an in-depth mechanistic understanding of the reaction was necessary. Conventional strategy generally needed designing tandem catalysts that possess both nitrate activation sites and hydrogenation sites to achieve high nitrate catalytic activity. For example, in our team's previous research, laser-controlled preparation of CuNi alloy as nitrate reduction electrocatalyst with tandem catalytic sites[17]. In which, the active hydrogen (H*) in the hydrogenation reaction typically came from water in the electrolyte. If there was insufficient active hydrogen available for the NIRR, it would limit the efficiency of converting NO_3^- to NH_3. Thus, designing an in-situ hydrogenation reaction on the electrocatalyst to improve the NIRR efficiency remains an area that required further research.

In general, titanium hydride had attracted attention for their ability as hydrogen storage material[21, 22]. Thomas F. Jaramillo employed titanium metal as the electrode for efficient electrochemical nitrate reduction to ammonia[23]. During the NIRR process, the titanium hydride was detected after long-time catalysis, but the contribution of titanium metal and titanium hydrides to the catalysis could not be determined. Additionally, other hydrogenation phenomena had also been observed in the electrochemical reduction of nitrate[24, 25]. Further, William A. Tarpeh reported that titanium hydrides exhibited excellent nitrate-catalytic activity and investigated the

catalyst structure in detail using GIXRD and XAS. They emphasized the importance of relating NIRR performance to the near-surface electrode structure to advance catalyst design and operation[26]. However, they believed that the reason for the high catalytic activity of hydrogenated titanium was attributed to the traditional proton-transfer mechanism (H* was derived from the electrolyte). So, the mechanism of lattice hydrogen participating in the hydrogenation catalytic reaction had not been proposed and confirmed.

In this work, the titanium hydride electrocatalyst synthesized by electrochemical hydrogenation reconstruction of titanium fiber paper. The obtained titanium hydride electrocatalyst exhibited an outstanding NH_3 yield rate of 83.64 mg h^{-1} cm^{-2} and FE of 99.11 % along with ampere-level current density of 1.05 A cm^{-2} at −0.7 V vs. RHE. We had confirmed the hydrogenation reaction involving lattice hydrogen during NIRR process through isotopic tracking experiments and theoretical calculations. The lattice hydrogen transfer mechanism was proposed, and the reversible equilibrium reaction between lattice hydrogen and active hydrogen (H*) was confirmed to not only improve the electrocatalytic activity of NIRR, but also demonstrate excellent catalytic stability. The more important matter was that the proposed mechanism of lattice hydrogen participating in the reversible catalytic reaction could be extended to other metal hydride, such as such as palladium hydride, tantalum hydride, and vanadium hydride. This understanding had provided a universal design concept for metal hydrides as catalysts and lattice hydrogen as H* sources for efficient

electrochemical NH_3 production, highlighting their potential for sustainable ammonia synthesis."

A collection of (some) other issues to address is given below:

1. In Fig. 1e, the author should provide the standard spectra of Ti, TiO_2 and TiH_2 and should be partially zoomed in to confirm the composition of the electrodes. And if possible, it would be desirable to conduct a separate XRD test of the $TiH_{1.97}$ on the electrode surface.

Response: Thank you for the reviewer's suggestion.

(1) According to the reviewers suggestions, we added the standard spectra of Ti (PDF# 44-1294), TiO_2 (PDF#71-1166), TiH_2 (PDF#09-0371) and $TiH_{1.97}$ (PDF#07-0370) in XRD spectrum to confirm the composition of the electrode (Fig. R7a), which clearly showed that our electrode could correspond well to the Ti (PDF# 44-1294) and $TiH_{1.97}$ (PDF#07-0370) standard spectra, indicating that the electrode was mainly composed of $TiH_{1.97}$ and Ti. Based on the XRD spectrum, it could be seen that apart from the characteristic diffraction peaks of $TiH_{1.97}$ and Ti, there were no other impurity diffraction peaks (such as titanium oxide and titanium nitride). In addition, we had partially zoomed in XRD spectrum at 39- 43° (Fig. R7b), which corresponded to the crystal face of $TiH_{1.97}$ (200), which further confirmed the chemical compositions in the electrode.

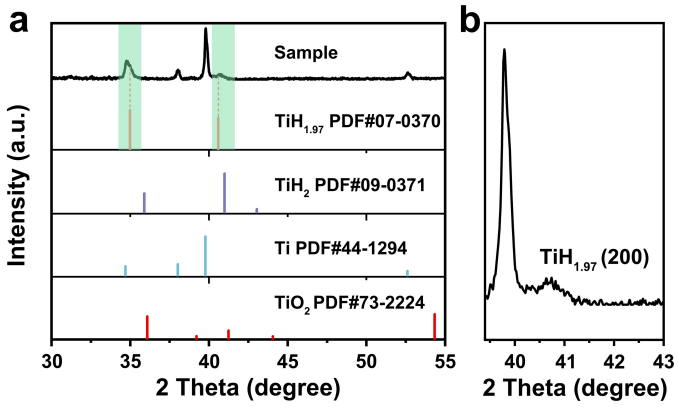

Fig. R7 (a) The XRD spectrum for electrode and the standard spectra of Ti (PDF# 44-1294), TiO_2 (PDF# 71-1166), TiH_2 (PDF# 09-0371) and $TiH_{1.97}$ (PDF# 07-0370). The magnified local image of the characteristic peak corresponding to **(b)** $TiH_{1.97}$ (200).

(2) we gently scraped off the black product from the electrode surface and performed XRD testing on it. From Fig. S5, it could be seen that the characteristic diffraction peaks of the material on the electrode surface could be well matched with $TiH_{1.97}$ (PDF#07-0370). Aside from these characteristic peaks, no other diffraction peaks were found, so we confirmed that the material on the electrode surface was pure $TiH_{1.97}$.

In the revised supporting information, we have added Fig. S5:

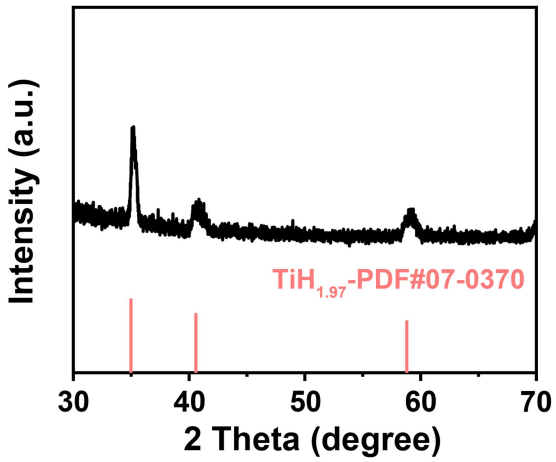

Fig. S5 A separate XRD test of the $TiH_{1.97}$ on the electrode surface.

2. The authors should provide SEM and TEM images of the original Ti FP. And The authors should provide SEM and TEM images of the $TiH_{1.97}$/Ti FP after electrocatalysis.

Response: We greatly appreciate the reviewer's good suggestion. We have provided SEM and TEM images of the original Ti FP and the $TiH_{1.97}$/Ti FP after electrocatalysis in Fig. S13. By comparing the morphology and structure of the electrodes before and after the NIRR reaction, we confirmed that the catalyst has good stability.

In the revised Supporting Information, we have added the Fig. S13 and the corresponding description as follows:

"Based on the SEM images in Fig. S13a and the locally magnified image (Fig. S13b), it could be seen that the Ti FP were formed by the intertwined and interwoven titanium fibers, and the diameter of a single titanium fiber was approximately 60 μm. The surface of the titanium fibers was smooth and free of any impurities. The TEM image (Fig. S13c) also showed the smooth surface and solid structure of the titanium fibers. After NIRR treatment, $TiH_{1.97}$/Ti still maintained the mesh-like structure of the titanium fiber paper (Fig. S13d), and the titanium hydride nanosheets on the surface did not undergo significant morphological changes compared to the pre-electrocatalysis (Fig. S13e and Fig. 1g). The TEM image (Fig. S13f) also showed that the surface of the nanosheets remained smooth after electrochemical catalysis, further indicating the good structural stability of the catalyst."

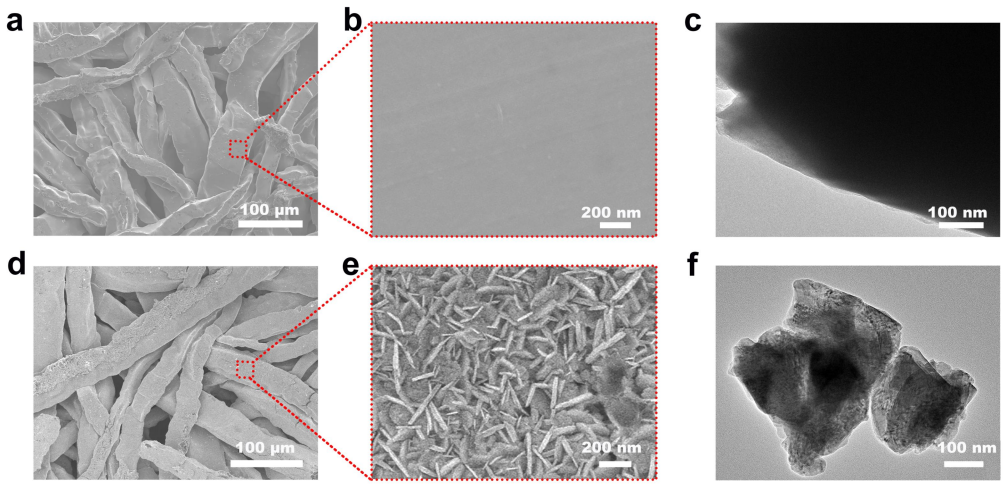

Fig. S13 (a, b) SEM and **(c)** TEM images of the original Ti FP. **(d, e)** SEM and **(f)** TEM images of the $TiH_{1.97}$/Ti FP after electrocatalysis.

3. In Fig. 2d, the author should provide the standard spectrum of TiH_2 (or $TiH_{1.97}$). The authors should clarify whether $TiH_{1.97}$ has lower or higher energy compared to Ti?

Response: Thanks to the comments. Inspired by reviewer's precious suggestion, we have provided the standard spectrum of TiH_2 and revised the XANES spectrum as illustrated in the Fig. 2d and Fig. 2e. In comparison to titanium, the pre-edge centroid of $TiH_{1.97}$ obviously shifted to higher energy than that of Ti. *(J. Am. Chem. Soc. 144, 5739-5744 (2022))*.

In the revised manuscript, we have modified Fig. 2d and Fig. 2e, the corresponding description as follows:

"The Ti K-edge XAFS spectra of $TiH_{1.97}$, standard spectrum of Ti and TiH_2 were presented in Fig. 2d. Unlike Ti, TiH_2 showed no pre-edge peak, indicating the near-surface structure of TiH_2 transitioned from the hexagonal packed structure of Ti to a face-centered cubic structure[26]. $TiH_{1.97}$ showed a pre-edge peak similar to that of the

TiH_2 but the energy was lower than that of TiH_2, indicating that $TiH_{1.97}$ had the same face-centered cubic structure as TiH_2 (Table S2). This difference also confirmed that the sample we obtained was $TiH_{1.97}$ rather than TiH_2. In addition, The Ti foil exhibited a significant Ti-Ti scattering peak at 2.52 Å, which shifted to 2.72 Å in $TiH_{1.97}$ in the Fourier transformed (FT-EXAFS), suggesting an increase in the Ti-Ti bond length after hydrogen introduction (Fig. 2e)."

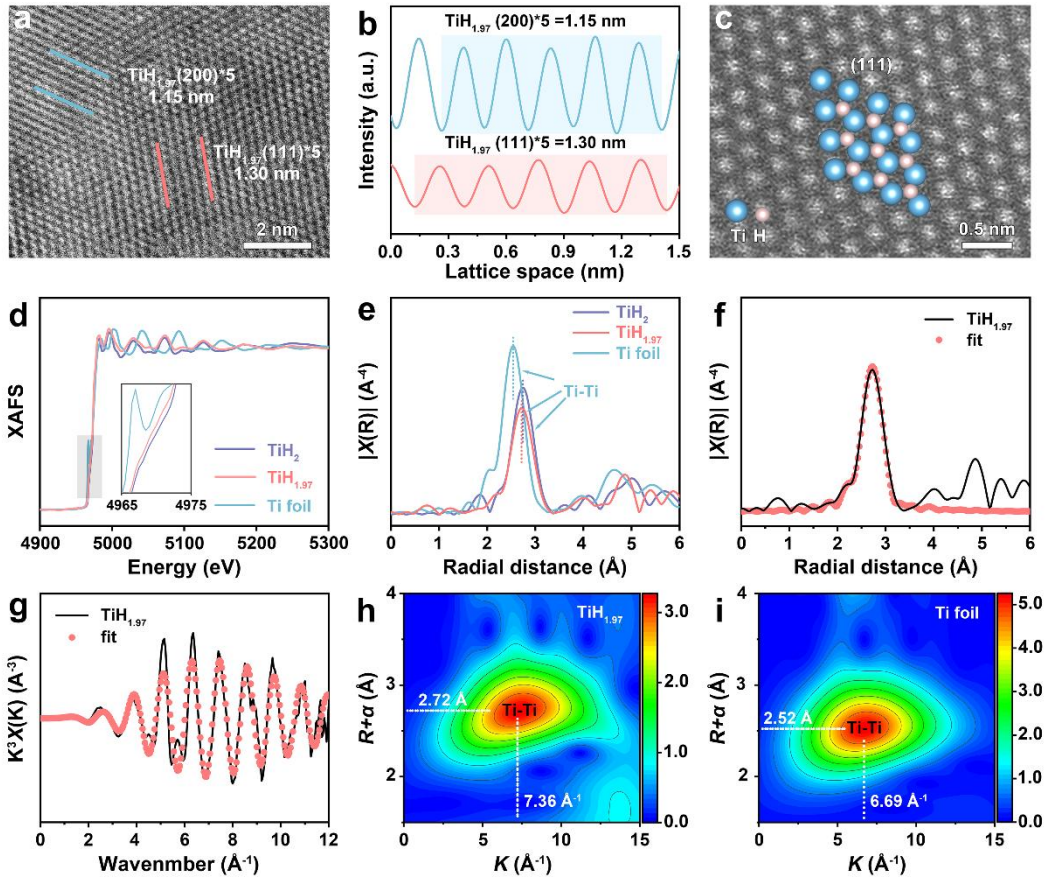

Fig. 2 (a) High-resolution HAADF-STEM image of titanium hydride. **(b)** Integrated pixel intensities in the selected regions of **(a)**. **(c)** Atomic-resolution HAADF-STEM image of titanium hydride **(d)** XAFS spectra and **(e)** FT-EXAFS spectra at Ti K-edge. **(f)** Ti K-edge EXAFS (line) and curve fit (points) for $TiH_{1.97}$ in R-space. **(g)** The fit curve of k3χ(k) oscillation functions in k-space for $TiH_{1.97}$. **(h, i)** WT-EXAFS of Ti for $TiH_{1.97}$ and Ti foil.

4. In Fig. S4, SAED pattern is not clear enough.

Response: We thank the reviewer for bringing up this point. The Fig. S4 has been changed to the Fig. S7, and we have replaced the SAED picture with a clearer one.

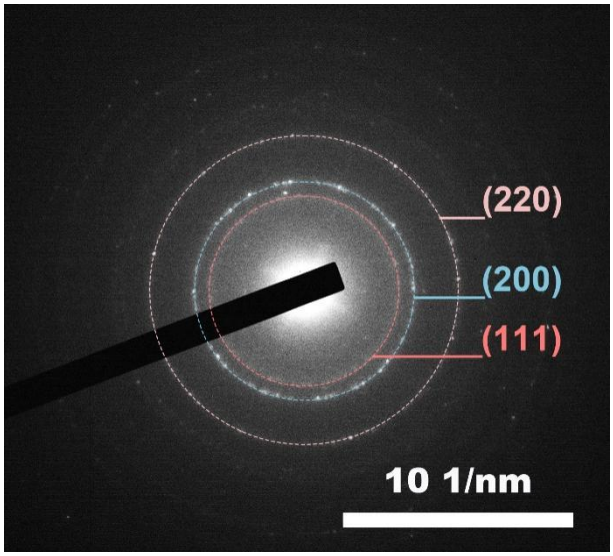

Fig. S7 SAED pattern of the titanium hydride.

5. In Fig. 3f, when comparing the performance of nitrate reduction, authors should use comparisons under similar conditions.

Response: Thank you for the reviewer's valuable suggestion. To verify that our catalyst has superior catalytic performance compared to other advanced catalysts, we had reviewed about 10 high-quality papers. Under the same test conditions (1M KOH + 0.1 M NO_3^-), their NH_3 yields and FE were compared in Fig. 3f. In addition, we had also compared our catalyst with other literature under the same concentration and the same potential, which also reflected the high catalytic activity of our catalyst (Fig. S16).

In the revised manuscript, we have modified Fig.3 f and the corresponding description as follows:

"Under the same conditions (1M KOH + 0.1 M NO_3^-), the titanium hydride catalyst demonstrated a significantly higher NH_3 yield rate (83.64 mg h^{-1} cm^{-2}) and FE (99.11%) at the potential of −0.7 V vs. RHE compared to the latest NIRR electrocatalysts documented in the literatures[15, 29, 30, 31, 32, 33, 34, 35, 36, 37], and the ECSA-normalized NH_3 yield up to 0.72, while maintaining NIRR performance that was on par with or superior to that of its competitors (Fig. 3f, Fig. S15, Table S3). In addition, the voltage ranges used in various literatures were different, and we also compared the NIRR performance under the same NO_3^- concentration with different voltage, our catalyst could achieve high FE and NH_3 yield rate over a wide voltage range as shown in Fig. S16, which was very important in ammonia synthesis, and this performance was difficult to achieve in other catalysts."

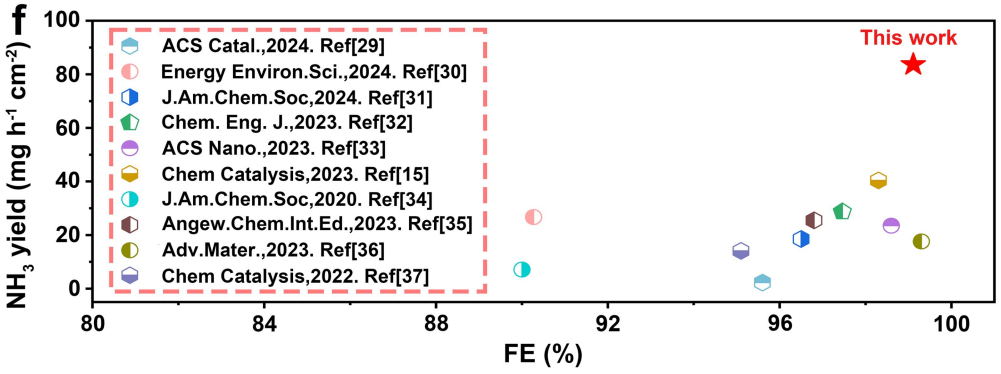

Fig. 3f Comparison of the NIRR performance of the titanium hydride with the reported electrocatalysts. (The nitrate concentrations of these reports were equal to 0.1 M).

In the revised Supporting Information, we added Fig. S16 and Table S3 as follow:

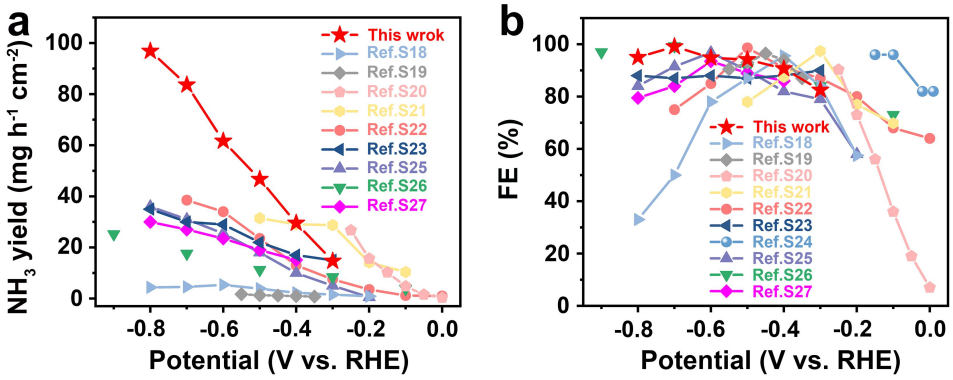

Fig. S16 The comparison of **(a)** NH_3 yields and **(b)** FE under different voltages with other literatures.

Table S3. The comparison of the NH_3 yield and FE with the reported catalysts for NIRR by the area of electrode and ECSA.

Catalyst	FE (%)	$Yied_{NH3}$ (mg h^{-1} cm^{-2})	ECSA (cm^2)	ECSA-normalized NH_3 yields	Electrolyte	Reduction Potential (vs. RHE)	Reference
$TiH_{1.97}$	99.1	**83.6**	115	**0.72**	1 M KOH + 0.1 M KNO_3	−0.7 V	This work
Cu_x S−$Co_{0.5}$	95.6	**2.3**	243	**0.01**	1 M KOH + 0.1 M KNO_3	−0.4 V	18
o-CoP/C@ Cu_3P/CF	90.3	**26.7**	1603	**0.01**	1 M KOH + 0.1 M KNO_3	−0.25 V	19
($Cu_{0.6}Co_{0.4}$) $C_{o2}O_4$	96.5	**18.5**	/	/	1 M KOH + 0.1 M NO_3^-	−0.45 V	20
CuO NWAs @Fe_3O_4	97.5	**28.7**	147	**0.19**	1 M KOH + 0.1 M KNO_3	−0.27 V	21
RuO_x/Pd	98.6	**23.5**	92	**0.24**	1 M KOH + 0.1 M KNO_3	−0.5 V	22
CNs@CoP	98.3	**40.4**	/	/	1 M KOH + 0.1 M $NaNO_3$	−0.60 V	23
$Cu_{50}Ni_{50}$	90.0	**7.1**	312	**0.02**	1 M KOH 0.1 M KNO_3	−0.15 V	24
FeB_2	96.8	**25.5**	123	**0.20**	1 M KOH + 0.1 M KNO_3	−0.6 V	25
Cu@C	99.3	**25.3**	587	**0.04**	1 M KOH + 0.1 M KNO_3	−0.7 V	26
CuFe-450	95.1	**14.1**	/	/	1 M KOH + 0.1 M KNO_3	−0.3 V	27

6. The author first proposed the concept of lattice hydrogen in the theoretical calculation part, but it seems that there is not much connection with the experimental part. Please further explain the relationship with the experimental part in detail.

Response: Thank you for the reviewer's valuable suggestion. First of all, the innovation of this paper lied in the promotion of nitrate reduction by lattice hydrogen transfer in titanium hydride, which were confirmed by both the isotope tracking experiments in Fig. 4a-c and theoretical calculation in Fig. 5.

(1) Connection to experimental observations:

① **The detail isotope tracking experiments** has been written in Supporting Information as follows:

Positive validation method for the participation of lattice hydrogen in hydrogenation reactions in titanium hydride. In an H-type electrolysis cell, a $TiH_{1.97}$/Ti catalyst was prepared. A D_2O solution containing 1 M NaOD and 0.1 M KNO_3 was used as the electrolyte for NIRR. Both the Ti FP and the synthesized $TiH_{1.97}$/Ti electrode were rinsed with D_2O for 10 minutes and dried at 250 ℃ under argon for 24 h to remove H_2O. NIRR was conducted at −0.7 V vs. RHE for 5 min, after which 10 mL of electrolyte was taken out and adjusted to pH = 4 with 2 M D_2SO_4, and the resulting products, NH_3 and ND_3, were explored using ^1H NMR.

Reverse validation method for the participation of lattice hydrogen in hydrogenation reactions in titanium hydride. In an H-type electrolysis cell, a $TiD_{1.97}$/Ti catalyst was prepared by cathodic electrochemical reconstruction for 30 min in a D_2O + NaOD + NO_3^- solution. Subsequently, an H_2O solution containing 1 M NaOH and 0.1 M

KNO_3 was used as the electrolyte for NIRR. NIRR was conducted at −0.7 V vs. RHE for 5 min, after which 10 mL of electrolyte was taken out and adjusted to pH = 4 with 2 M D_2SO_4, and the resulting products, NH_3 and ND_3, were explored using ^1H NMR. In order to more intuitively understand the process of isotope tracking experiment, we have added the flow chart as below:

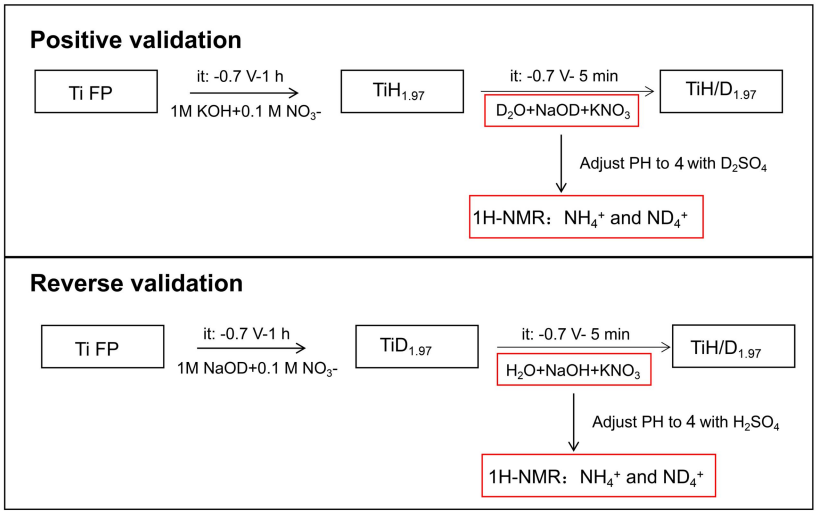

② **Isotope tracking experiments result analysis:** To reveal the reaction mechanism for enhancing NIRR catalytic activity, isotope tracking experiments were used to investigate the electrochemical behavior of lattice hydrogen transfer from titanium hydride. The model diagram for the positive and reverse verification of isotope-labeled lattice hydrogen transfer during the NIRR process was shown in Fig. 4a. For the positive verification, titanium and titanium hydride serving as electrocatalysts and using 1 M NaOD + 0.1 M KNO_3 in D_2O solution as the electrolyte for NIRR, the peaks at 7.05, 7.14 and 7.23 ppm in the ^1H NMR spectrum of Ti were identified as the characteristic peaks of ND_4^+. In the ^1H NMR spectrum of titanium hydride, besides the characteristic peaks of ND_4^+, a set of typical peaks for

NH_4^+ at 7.03, 7.12, and 7.20 ppm was observed, which were attributed to the lattice hydrogen in $TiH_{1.97}$ (Fig. 4b). In the reverse verification, using the same method, we synthesized the $TiD_{1.97}$ catalyst (The XRD and solid-state NMR spectra used to confirm the successful synthesis of $TiD_{1.97}$ were shown in Fig. S18) and used 1 M NaOH + 0.1 M KNO_3 in H_2O solution as the electrolyte for NIRR. In the ^1H NMR spectrum of $TiD_{1.97}$, in addition to the characteristic peaks of NH_4^+, the typical peaks of ND_4^+ were also noted, indicating their origin from lattice deuterium in $TiD_{1.97}$ (Fig. 4c). Through the aforementioned positive and reverse verification, we had concluded that the lattice hydrogen in titanium hydride indeed participated in the hydrogenation reaction of NIRR. Lattice hydrogen effused from titanium hydride and was converted into H*, while the H* in the solution ensures the formation of titanium hydride. The reversible equilibrium reaction between lattice hydrogen and H* not only enhanced the electrocatalytic activity of NIRR but also exhibited excellent catalytic stability.

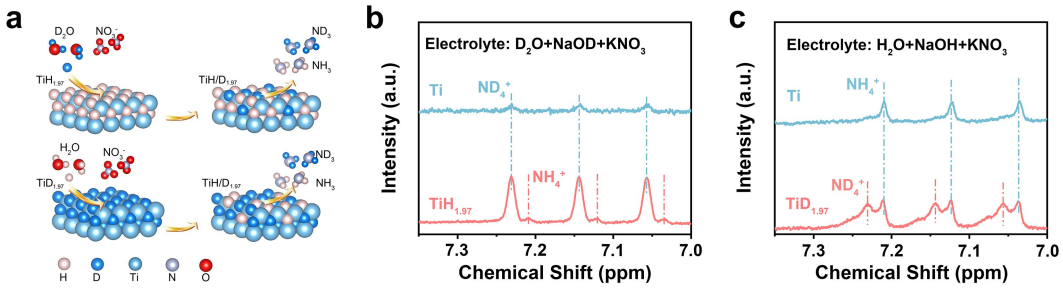

Fig. 4 (a) Model diagrams for positive and reverse validation of Isotope labeled lattice hydrogen transfer in NIRR process. **(b)** Isotope labeled lattice hydrogen transfer in NIRR process for $TiH_{1.97}$ (positive validation) and **(c)** $TiD_{1.97}$ (reverse validation).

(2) Theoretical calculation on lattice hydrogen:

The theoretical computation part serves as the foundation for the experiment. In the theoretical part, we conducted computational modeling and simulation of NIRR of $TiH_{1.97}$ to explore the lattice hydrogen transfer mechanism. First of all, Density Functional Theory (DFT) calculations had revealed the competitive behavior between different sources of H* during the hydrogenation process of NIRR (one was from water splitting, the other was from the lattice hydrogen in $TiH_{1.97}$). Fig. 5b illustrated the competitive dynamics between the adsorption of H* from different sources during the initial protonation stage of NIRR. The calculated reaction energy barriers for the transformation of $*NO_3$ to $*NO_3H$ using H* derived from H_2O and lattice hydrogen were 0.68 eV and 0.31 eV, respectively. As a results, we could conclude that lattice hydrogen would preferentially participate in the NIRR rather than the H* from the H_2O solution. In addition, when lattice hydrogen overflows in $TiH_{1.97}$ to form an H vacancy ($TiH_{1.97}$-H_v), it exhibited a relatively strong ability to adsorb H*. Therefore, $Tih_{1.97}$-H_V could absorb H* produced by H_2O cracking, thus forming $TiH_{1.97}$. The dynamic balance between the formation and consumption of H* in $TiH_{1.97}$ ensured the high efficiency of nitrate reduction.

(3) Therefore, through isotope tracking experiments and theoretical calculations, we had proven that the H* produced in the titanium hydride lattice hydrogen was more likely to participate in the hydrogenation reaction of NIRR, and the H* generated by water electrolysis timely replenishes the consumption of lattice hydrogen in titanium hydride. The dynamic balance between the generation and consumption of this H*

ensured the high activity of nitrate reduction. The results of theoretical calculations further confirmed the conclusions of our experiments.

7. Incorrect captions for Fig. 3e, Fig. 3f and Fig. 3g.

Response: We would thank for the reviewer's valuable comments and suggestions. According to the reviewer's suggestion, all the captions of Fig. 3e, Fig. 3f and Fig. 3g had been carefully check and corrected in the revised manuscript.

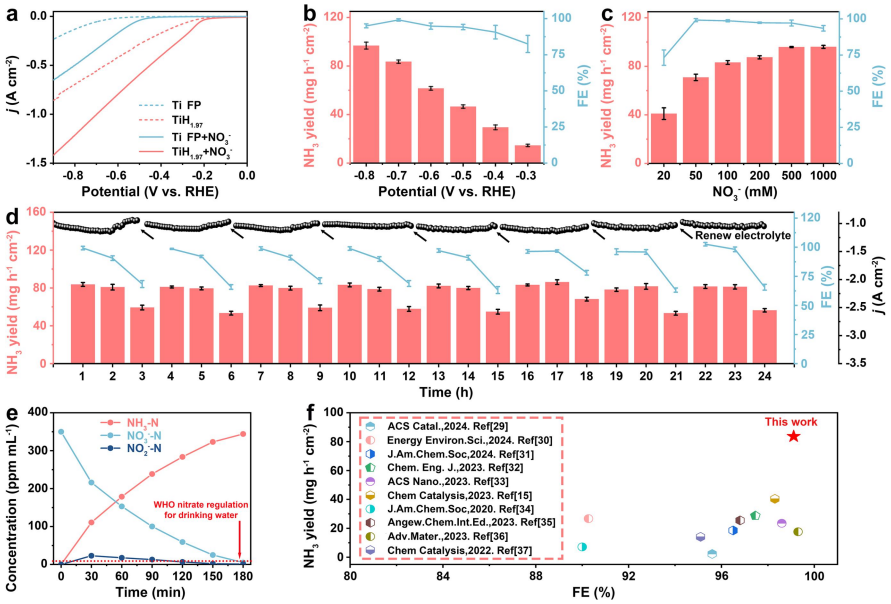

Fig. 3 (a) LSV curves of Ti FP and titanium hydride with and without NO_3^-. **(b)** NH_3 yields and FEs for titanium hydride against various work potentials in 1 M KOH solution with 0.1 M NO_3^-. **(c)** NH_3 yields and FEs for titanium hydride at different concentrations of NO_3^-. **(d)** Stability test at −0.7 V vs. RHE with periodic updates taken every 3 h. **(e)** Time-dependent concentration change of NO_3^--N, NO_2^--N and NH_3-N. **(f)** Comparison of the NIRR performance of the titanium hydride with the reported electrocatalyst (The nitrate concentrations of these reports are equal to 0.1 M).

8. Could the authors explain what is the proportion of Ti converted to $TiH_{1.97}$ on the electrode surface? According to the XRD pattern, it seems that some Ti still exists. The authors need more characterization to verify the composition of the electrode surface.

Response: Thank you very much for your professional questions, which is very helpful to improve the quality of our paper. According to the reviewer's suggestion, we have determined the proportion of Ti converted to titanium hydride on the electrode surface was ~ 1 % (wt %) though weighing the difference in mass before and after the reaction, as follow:

(1) Weighing the difference in mass before and after the reaction:

To calculate the weight fraction of the titanium hydride catalyst on the electrode surface, we calculated the loading amount of titanium hydride catalyst on the electrode. We used the strong oxidizing agent (HCl: 0.1 M) to undergo a chemical reaction with the electrode ($TiH_{1.97}$/Ti). By weighing the difference in mass before and after the reaction (Fig. S4), we could obtain the weight of the titanium hydride loaded on the electrode (data from five sets of measurements were taken and the average was calculated). This was because metal hydrides were highly reactive with HCl, while metallic titanium did not react with HCl, so the weight loss on the electrode belongs to titanium hydride. Through calculation, we obtained a $TiH_{1.97}$ loading of 0.6 mg cm^{-2} on the electrodes and the weight fraction of titanium hydride on the electrode surface was ~ 1 % (wt %).

We have added **Fig. S4** in the supporting information to get the loading of titanium hydride as flow:

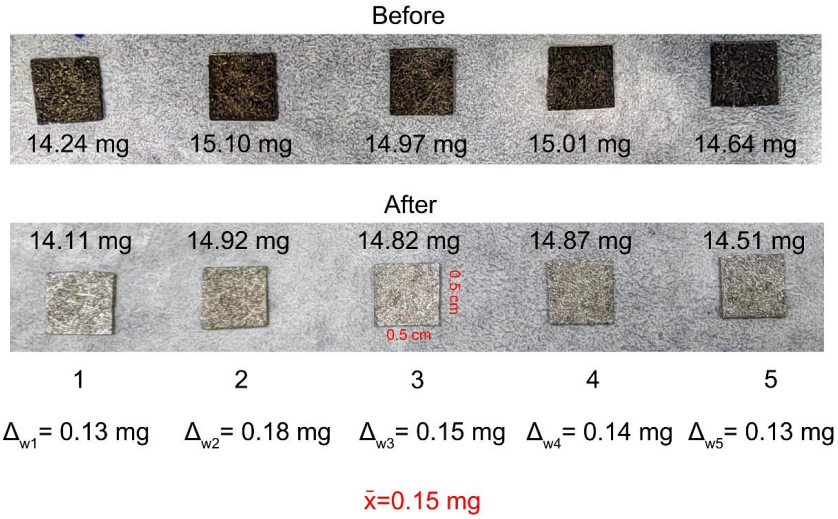

Fig. S4 Weighing the difference in mass before and after the reaction

(2) XPS Analysis:

In addition, to study the chemical state of the electrode surface, the argon ion etching XPS was employed. Etching was conducted in the same region of the same sample for a total duration of 1000 s (40 nm). Fig. R8 showed the changes in the Ti 2p spectrum under the etching conditions, which clearly saw that when the etching depth was 30 nm and 40nm (Fig. R8 e, f), there was an obvious Ti^0 signal peak, indicating that the thickness of titanium hydride on the electrode surface was ~30 nm.

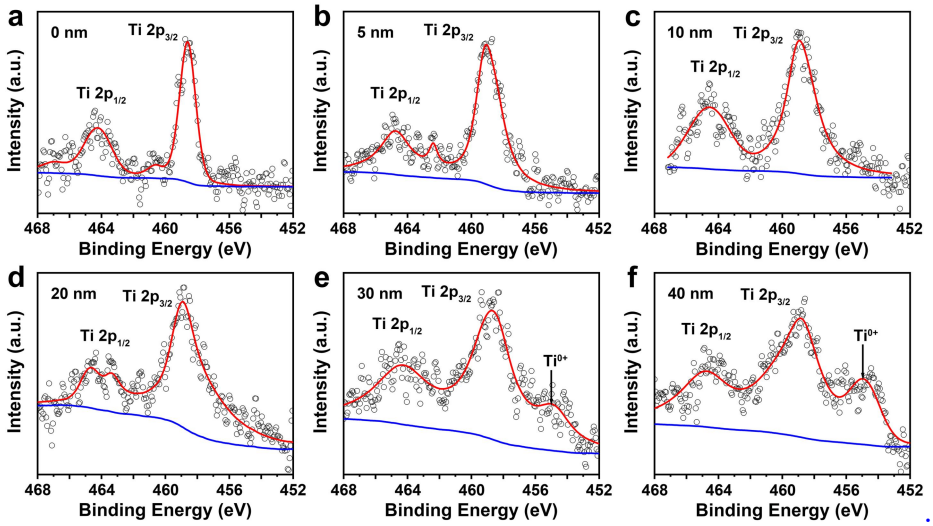

Fig. R8 XPS spectra of Ti 2p region for titanium hydride with different sputtering depths.

Reviewer #4 (Remarks to the Author):

This work demonstrated the electrochemical synthesis of titanium hydride from Ti fiber paper and reported its exceptional catalytic performance for electrochemical nitrate reduction reaction to ammonia (NIRR). The involvement of lattice hydrogen in the titanium hydride in the catalysis to provide protons to the produced ammonia was proposed and confirmed both experimentally and computationally. Other metal hybrids were also briefly tested for NIRR. Lots of experiments have been systematically conducted to make most findings and conclusions promising. The authors have done lots of work and organized the results into a well-written manuscript, and the work presented here is indeed interesting. However, the novelty of this work is not sufficient for Nature Communications. As indicated in the following specific comment (#1), the use of electrochemically synthesized titanium hydride for NIRR as well as the involvement of hydrogen from the titanium hydride during the catalysis have been already reported previously, but unfortunately, the authors did not mention this fact in the manuscript. Thus, I cannot recommend the publication of this work in Nature Communications. Since this is indeed a solid work with nice catalytic performances and experimental investigations on the proton-transfer mechanism, although its major novelty and impact were already published previously, this work may be published in a more specialized journal in the fields of fundamental catalysis or physical chemistry, after the following comments are addressed.

Response: Thank you very much for the valuable comments and suggestions provided by the reviewer. We regret that we were not to make a reasonable comparison between our work and the main innovations of the previously published research, which was an omission and deficiency in our work. We had made the relevant revisions in the article. Regarding the reviewers' concerns about the Since this was indeed a solid work with nice catalytic performances and experimental investigations on the proton-transfer mechanism," issue, I think **the reviewer had confused the lattice hydrogen participation mechanism in the reaction mechanism of this paper with the traditional active hydrogen transfer mechanism.** I will elaborate on the proposed active hydrogen transfer mechanism and its innovativeness from the following aspects:

(1) In fact, Jaramillo and coworkers in 2020 *(ACS Sustain. Chem. Eng. 8, 2672-2681 (2020))* reported that by controlling electrolyte conditions at a titanium electrode, high selectivity for ammonia production could be achieved via electroreduction of nitrates. During the NIRR process, titanium hydride was detected after prolonged catalysis, **but the contributions of metallic titanium and titanium hydride to the catalysis could not be conclusively determined.**

Tarpeh and coworkers investigated the role of electrochemically synthesized TiHx ($0 < x \leq 2$) in NIRR in 2022 *(J. Am. Chem. Soc. 144, 5739-5744 (2022))*. The NIRR on titanium surfaces leaded to significant surface reconstruction and the formation of titanium hydrides (TiHx, $0<x<2$). They used ex-situ GIXRD and XAS demonstrated that the near-surface TiH_2 phase became more enriched as the applied potential and

duration of the NIRR increase. This work emphasized the importance of relating NIRR performance to the near-surface electrode structure to advance catalyst design and operation. **High-activity TiH_x catalysts had been reported, but the catalytic mechanism was still based on the traditional proton-transfer mechanism that the H* was derived from the electrolyte not the lattice hydrogen transfer mechanism. The structure-activity relationship of TiH_x catalysts had been discussed, but the mechanism of lattice hydrogen participation in the hydrogenation process had not been proposed.**

(2) In our manuscript, the primary innovation lied in the participation of lattice hydrogen in the hydrogenation reaction of NIRR, this viewpoint differed from the traditional mechanism that proton transfer mechanism of the active hydrogen generated in the water, which had not been explored in previous studies. And we had verified this conclusion through **isotopic tracking experiments (Fig. 4a-c)** and **theoretical calculations (Fig. 5)**, which was the core innovation of our paper.

Isotope tracking experiments results analyse:

To reveal the reaction mechanism for enhancing NIRR catalytic activity, isotope tracking experiments were used to investigate the electrochemical behavior of lattice hydrogen transfer from titanium hydride. The model diagram for the positive and reverse verification of isotope-labeled lattice hydrogen transfer during the NIRR process was shown in Fig. 4a. For the positive verification, titanium and titanium hydride serving as electrocatalysts and using 1 M NaOD + 0.1 M KNO_3 in D_2O solution as the electrolyte for NIRR, the peaks at 7.05, 7.14 and 7.23 ppm in the ^1H

NMR spectrum of Ti were identified as the characteristic peaks of ND_4^+. In the ^1H NMR spectrum of titanium hydride, besides the characteristic peaks of ND_4^+, a set of typical peaks for NH_4^+ at 7.03, 7.12, and 7.20 ppm was observed, which were attributed to the lattice hydrogen in titanium hydride (Fig. 4b). In the reverse verification, using the same method, we synthesized the $TiD_{1.97}$ catalyst (The XRD and solid-state NMR spectra used to confirm the successful synthesis of $TiD_{1.97}$ were shown in Fig. S18) and used 1 M NaOH + 0.1 M KNO_3 in H_2O solution as the electrolyte for NIRR. In the ^1H NMR spectrum of $TiD_{1.97}$, in addition to the characteristic peaks of NH_4^+, the typical peaks of ND_4^+ were also noted, indicating their origin from lattice deuterium in $TiD_{1.97}$ (Fig. 4c). Through the aforementioned positive and reverse verification, we had concluded that the lattice hydrogen in titanium hydride indeed participated in the hydrogenation reaction of NIRR. Lattice hydrogen effused from titanium hydride and was converted into H*, while the H* in the solution ensures the formation of titanium hydride. The reversible equilibrium reaction between lattice hydrogen and H* not only enhanced the electrocatalytic activity of NIRR but also exhibited excellent catalytic stability.

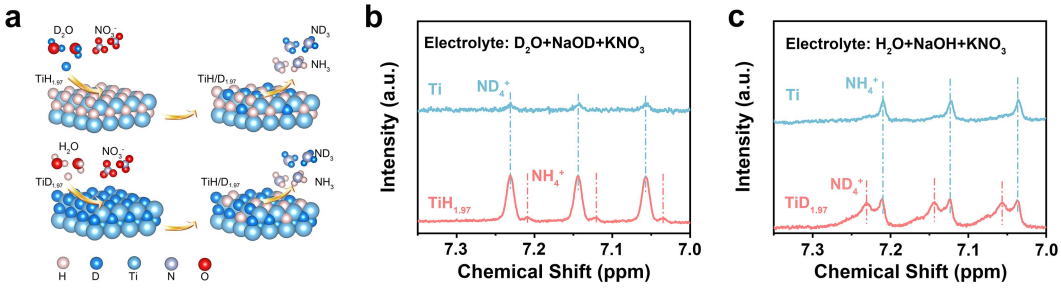

Fig. 4 (a) Model diagrams for positive and reverse validation of Isotope labeled lattice hydrogen transfer in NIRR process. **(b)** Isotope labeled lattice hydrogen transfer in NIRR process for $TiH_{1.97}$ (positive validation) and **(c)** $TiD_{1.97}$ (reverse validation).

(3) More importantly, the proposed mechanism of lattice hydrogen participating in catalytic reversible reactions could be extended to other metal hydrides, such as **palladium hydride (Fig. S24), tantalum hydride (Fig. S25), and vanadium hydride (Fig. S26)**. Additionally, this mechanism of lattice hydrogen facilitating catalytic reactions might also have implications for other hydrogenation reactions, such as the hydrogenation of carbon dioxide.

(4) Overall, the main innovation and breakthrough of our research compared to previous studies lied in the fact that we had clearly elucidated the reversible equilibrium reaction between lattice hydrogen and active hydrogen in titanium hydride as the key to enhancing NIRR performance. This finding provided a universal design principle for metal hydrides as effective electrochemical ammonia synthesis catalysts, highlighting their potential in sustainable ammonia synthesis. The proposed mechanism injects new vitality into the understanding of the microscopic mechanism of hydrogen electrochemical catalysis reactions, and also provided a new direction for expanding the horizon of hydrogen electrocatalyst.

(5) In the revised draft, we have carefully reviewed the relevant literature and appropriately cite and discuss these important previous works in the text. Thank you again for the valuable feedback. We would take these comments seriously and strive to submit an even more refined revised version.

1. *As mentioned in the general comment, the use of titanium hydride electrochemically generated from metallic Ti electrodes for NIRR was first reported by Jaramillo and coworkers in 2020 (ACS Sustainable Chem. Eng. 2020, 8, 7, 2672–2681), and Tarpeh and coworkers investigated the role of electrochemically synthesized TiHx ($0 < x \leq 2$) in NIRR in 2022 (J. Am. Chem. Soc. 2022, 144, 13, 5739–5744). The involvement of hydrogen from the titanium hydride during the NIRR, which is the main point proposed in this work, was also proposed and computationally investigated in the 2022 JACS paper. However, the authors did not mention any of them in the manuscript. The former was not even cited, and the authors only cited the latter one for indexing the crystalline lattice of TiHx without mentioning the contributions of the previous work. This is not acceptable for a work submitted to Nature Communications, as the authors were not able to justify the major novelty of their work compared to published studies.*

Response: Thank you for the reviewer's suggestions, we have made corresponding revisions to the manuscript based on these suggestions.

(1) First, we sincerely apologized for not including the references mentioned by the reviewer in the manuscript. We had revisited and reorganized the introduction section in the manuscript.

(2) We carefully reviewed the literature cited by the reviewers and found that the viewpoints we proposed were completely different from the viewpoints described in the literature.

① Jaramillo and coworkers in 2020 *(ACS Sustain. Chem. Eng. 8, 2672-2681*

(2020)) reported that by controlling electrolyte conditions at a titanium electrode, high selectivity for ammonia production could be achieved via electroreduction of nitrates. During the NIRR process, titanium hydride was detected after prolonged catalysis, **but the contribution of titanium metal and titanium hydrides to the catalysis could not be determined**.

The original text was as follows:

> hydrogen absorption into the Ti lattice rather than production of hydrogen gas on a fresh Ti electrode and that, in general, increasing the nitrate concentration increasingly suppresses the HER. Because it is known that Ti immediately forms a surface hydride layer in acidic solutions under low cathodic potentials, it is ultimately unclear whether the active catalyst in our system is Ti, Ti hydride, or a combination of species. Thus, we cannot rule out the possibility that the degradation of the FE in the 8 h stability test (Figure 3B) could be influenced by the presence of TiH_x. Determining the structure of the active catalyst under different conditions and the effects of the resulting active sites on catalyst properties will be an important long-term goal in gaining a complete understanding of this system.

② Tarpeh and coworkers investigated the role of electrochemically synthesized TiHx ($0 < x \leq 2$) in NIRR in 2022 *(J. Am. Chem. Soc. 144, 5739-5744 (2022))*. The NIRR on titanium surfaces leaded to significant surface reconstruction and the formation of titanium hydrides (TiHx, $0<x<2$). They used ex-situ GIXRD and XAS demonstrated that the near-surface TiH_2 phase became more enriched as the applied potential and duration of the NIRR increase. This work emphasized the importance of relating NIRR performance to the near-surface electrode structure to advance catalyst design and operation. **High-activity TiH_x catalysts had been reported, but the**

catalytic mechanism was still based on the traditional proton-transfer mechanism that the H* was derived from the electrolyte not the lattice hydrogen transfer mechanism. The structure-activity relationship of TiH_x catalysts had been discussed, but the mechanism of lattice hydrogen participation in the hydrogenation process had not been proposed. Regarding the reviewers' concerns about the " Since this is indeed a solid work with nice catalytic performances and experimental investigations on the proton-transfer mechanism," issue, the reviewer had confused the lattice hydrogen participation mechanism in the reaction mechanism of this paper with the traditional active hydrogen transfer mechanism.

(3) To clarify the mechanism of hydrogenation reactions involving lattice hydrogen, we have reorganized the development process of titanium hydride electrocatalyst in the introduction:

"In order to rationally design NIRR catalysts, an in-depth mechanistic understanding of the reaction was necessary. Conventional strategy generally needed designing tandem catalysts that possess both nitrate activation sites and hydrogenation sites to achieve high nitrate catalytic activity. For example, in our team's previous research, laser-controlled preparation of CuNi alloy as nitrate reduction electrocatalyst with tandem catalytic sites[17]. In which, the active hydrogen (H*) in the hydrogenation reaction typically came from water in the electrolyte. If there was insufficient active hydrogen available for the NIRR, it would limit the efficiency of converting NO_3^- to NH_3. Thus, designing an in-situ hydrogenation reaction on the electrocatalyst to improve the NIRR efficiency remains an area that required further research.

In general, titanium hydride had attracted attention for their ability as hydrogen storage material[21, 22]. Thomas F. Jaramillo employed titanium metal as the electrode for efficient electrochemical nitrate reduction to ammonia[23]. During the NIRR process, the titanium hydride was detected after long-time catalysis, but the contribution of titanium metal and titanium hydrides to the catalysis could not be determined. Additionally, other hydrogenation phenomena had also been observed in the electrochemical reduction of nitrate[24, 25]. Further, William A. Tarpeh reported that titanium hydrides exhibited excellent nitrate-catalytic activity and investigated the catalyst structure in detail using GIXRD and XAS. They emphasized the importance of relating NIRR performance to the near-surface electrode structure to advance catalyst design and operation[26]. However, they believed that the reason for the high catalytic activity of hydrogenated titanium was attributed to the traditional proton-transfer mechanism (H* was derived from the electrolyte). So, the mechanism of lattice hydrogen participating in the hydrogenation catalytic reaction had not been proposed and confirmed.

In this work, the titanium hydride electrocatalyst synthesized by electrochemical hydrogenation reconstruction of titanium fiber paper. The obtained $TiH_{1.97}$ electrocatalyst exhibited an outstanding NH_3 yield rate of 83.64 mg h^{-1} cm^{-2} and FE of 99.11% along with ampere-level current density of 1.05 A cm^{-2} at −0.7 V vs. RHE. We had confirmed the hydrogenation reaction involving lattice hydrogen during NIRR process through isotopic tracking experiments and theoretical calculations. The lattice hydrogen transfer mechanism was proposed, and the reversible equilibrium

reaction between lattice hydrogen and active hydrogen (H*) was confirmed to not only improve the electrocatalytic activity of NIRR, but also demonstrate excellent catalytic stability. The more important matter was that the proposed mechanism of lattice hydrogen participating in the reversible catalytic reaction could be extended to other metal hydride, such as such as palladium hydride, tantalum hydride, and vanadium hydride. This understanding had provided a universal design concept for metal hydrides as catalysts and lattice hydrogen as H* sources for efficient electrochemical NH_3 production, highlighting their potential for sustainable ammonia synthesis."

2. The use of other metal hydrides in NIRR was also reported by others in early studies (Electrochimica Acta, 52 (2006) 1329-1338; Journal of Electroanalytical Chemistry, 599 (2007) 167-176), thus the authors should mention and cite them.

Response: Thanks to the comments. Inspired by the reviewer's valuable advice, we have carefully read the literature on the study of hydrides in NIRR (*Electrochim Acta. 52, 1329-1338 (2006).*; *J. Electroanal. 599, 167-176 (2007)*), and quoted these references in the introduction section as 24, 25. It was worth noting that these hydrides were not used as electrocatalysts for NIRR but were observed to form on the electrode surface during the process where metals act as electrocatalysts for NIRR. The contribution of metal electrodes and hydrides to NIRR as well as the catalytic mechanism has not been studied.

3. How did the authors determine the number "1.97" in the molecular formula? No solid proof was found in the manuscript. Without solid proof, TiHx or TiH_2 may be more appropriate.

Response: Thank you very much for your professional questions, which are very helpful to improve the quality of our paper.

(1) Inspired by the reviewer's valuable advice, we provided the standard cards for Ti (PDF#44-1294), $TiH_{1.97}$ (PDF#07-0370), TiO_2 (PDF#71-1166), and TiH_2 (PDF#09-0371) (Fig. R7a), and partially magnify the diffraction peaks at 39-43° (Fig. R7b). By comparison, we found that the chemical compositions of electrode was composed of Ti and $Ti_{1.97}$, and moreover, there were no characteristic peaks of other impurities such as TiO_2 in the XRD pattern. Furthermore, since the standard card of TiH_2 had a slightly larger shift in peak position compared to our sample, we believed that it was more appropriate to name it $TiH_{1.97}$.

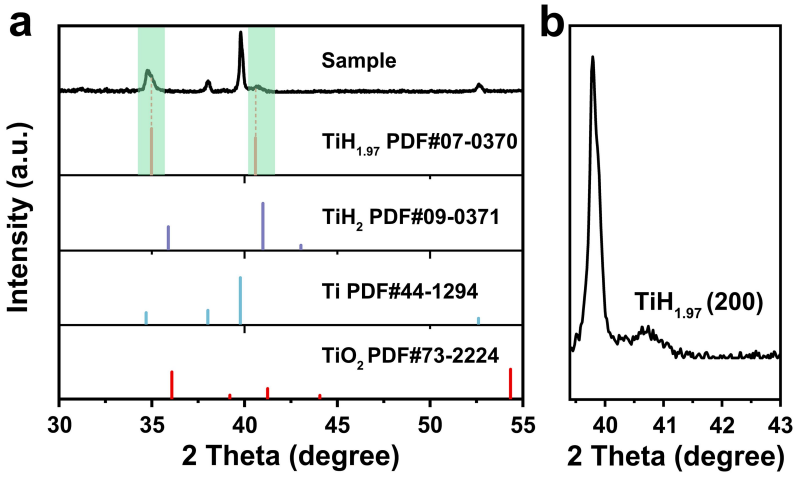

Fig. R7 (a) The XRD spectrum for electrode and the standard spectra of Ti (PDF# 44-1294), TiO_2 (PDF# 71-1166), TiH_2 (PDF#09-0371) and $TiH_{1.97}$ (PDF#07-0370) and (b) partially magnify the diffraction peaks at 39-43°.

In addition, in order to more intuitively see the diffraction peaks on the electrode surface belonging to $TiH_{1.97}$, we provide the detailed information of the standard card (PDF#07-0370) of $TiH_{1.97}$ (Fig. R9), as shown in the following:

PDF#07-0370: QM=Intermediate; d=Film/Visual; I=(Unknown)
Titanium Hydride
TiH1.971
Radiation=CuKa1 Lambda=1.5406 Filter=
Calibration= 2T=34.981-128.842 I/Ic(RIR)=
Ref: Level-1 PDF

Cubic, Fm-3m(225) Z=4 mp=
CELL: 4.44 x 4.44 x 4.44 <90.0 x 90.0 x 90.0> P.S=
Density(c)=3.94 Density(m)= Mwt= Vol=87.5
Ref: Ibid.

Strong Lines: 2.56/X 2.22/8 1.57/7 1.34/7 0.85/7 1.02/6 0.99/6 0.91/6

2-Theta	d(?)	I(f)	(h k l)	Theta	1/(2d)	2pi/d	n^2
34.981	2.5630	100.0	(1 1 1)	17.490	0.1951	2.4515	3
40.587	2.2210	80.0	(2 0 0)	20.293	0.2251	2.8290	4
58.806	1.5690	70.0	(2 2 0)	29.403	0.3187	4.0046	8
70.238	1.3390	70.0	(3 1 1)	35.119	0.3734	4.6924	11
73.930	1.2810	30.0	(2 2 2)	36.965	0.3903	4.9049	12
87.691	1.1120	10.0	(4 0 0)	43.845	0.4496	5.6503	16
98.215	1.0190	60.0	(3 3 1)	49.107	0.4907	6.1660	19
101.743	0.9930	60.0	(4 2 0)	50.871	0.5035	6.3275	20
116.471	0.9060	60.0	(4 2 2)	58.236	0.5519	6.9351	24
128.842	0.8540	70.0	(5 1 1)	64.421	0.5855	7.3574	27

Fig. R9 The detailed information of the standard card (PDF#07-0370) of $TiH_{1.97}$

In the revised manuscript, we have modified the Fig.1e as follows: “

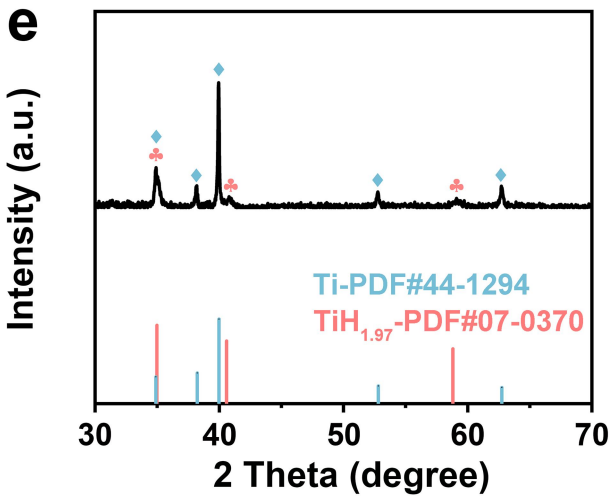

Fig. 1 (e) XRD spectrum.

(2) we gently scraped off the black product from the electrode surface and performed XRD testing on it. From Fig. S5, it could be seen that the characteristic diffraction peaks of the material on the electrode surface could be well matched with $TiH_{1.97}$ (PDF#07-0370). Aside from these characteristic peaks, no other diffraction peaks were found, so we confirmed that the material on the electrode surface was pure $TiH_{1.97}$.

In the revised Supporting information, we have added Fig. S5 as follows:

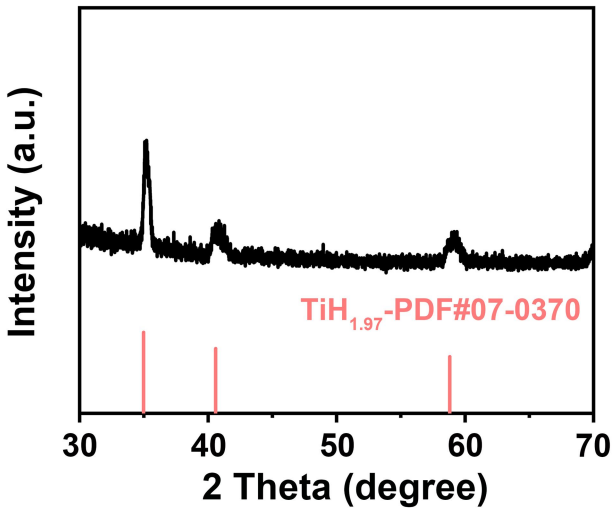

Fig. S5 A separate XRD test of the $TiH_{1.97}$ on the electrode surface.

(3) We also provided the standard spectrum of TiH_2 and revised the XANES spectrum as illustrated in the Fig. 2d and Fig. 2e. $TiH_{1.97}$ showed a pre-edge peak similar to that of the TiH_2 but the energy was lower than that of TiH_2, indicating that $TiH_{1.97}$ had the same face-centered cubic structure as TiH_2 (Table S2). This difference also confirmed that the sample we obtained was $TiH_{1.97}$ rather than TiH_2.

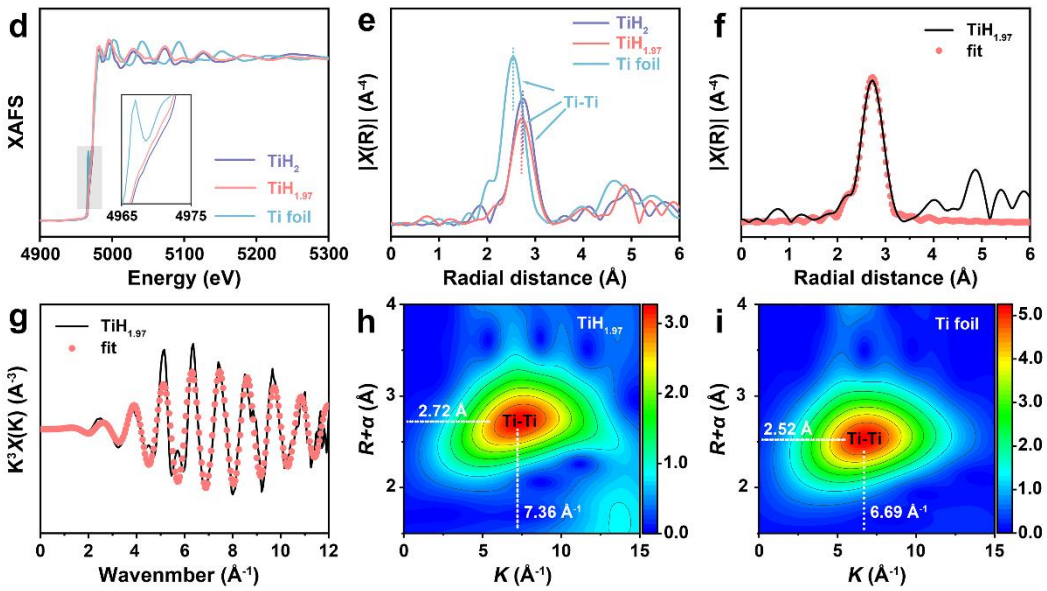

Fig. 2 **(d)** XAFS spectra and **(e)** FT-EXAFS spectra at Ti K-edge. **(f)** Ti K-edge EXAFS (line) and curve fit (points) for $TiH_{1.97}$ in R-space. **(g)** The fit curve of k3χ(k) oscillation functions in k-space for $TiH_{1.97}$. **(h, i)** WT-EXAFS of Ti for $TiH_{1.97}$ and Ti foil.

4. In addition, following the previous comment, is there any change in the ratio between titanium and hydrogen in the catalyst during the electrocatalysis? If the lattice hydrogen did involve in the electrocatalysis according to the authors' isotope experiments, the formula of the material might change.

Response: Thank you for your valuable advice. In titanium hydride, the overflowing of lattice hydrogen formed H* and participated in the hydrogenation reaction during the nitrate reduction process, while the H* generated by water electrolysis replenishes the hydrogen consumption in titanium hydride. The dynamic equilibrium process of this hydrogen consumption and replenishment was the main point of our article, which were confirmed by both the isotope tracking experiments in Fig. 4a-c and

theoretical calculation in Fig. 5. Based on the viewpoints we had put forward, the ratio of Ti and H would not change during the NIRR process.

(1) To verify our viewpoint, we tested XRD spectrum of electrode during NIRR at applied potentials of −0.1, −0.2, −0.4, −0.6 and −0.8 V vs. RHE. As could be seen from the ex-situ XRD pattern (Fig. S14), the phase of $TiH_{1.97}$ did not change during the NIRR process, which meant that the ratio of Ti and H in the active material titanium hydride remained unchanged. This result also confirmed the correctness of the hydrogen dynamic equilibrium we proposed.

In the revised manuscript, we had added the corresponding description as follows:

"We also tested the XRD spectrum of electrode during NIRR at applied potentials of −0.1, −0.2, −0.4, −0.6 and −0.8 V vs. RHE. Based on ex-situ XRD patterns (Fig. S14), the phase of titanium hydride did not change during the NIRR process, indicating that the Ti to H ratio in the active material remained unchanged. This result also confirmed our proposed viewpoint: during the NIRR process, the H in the titanium hydride lattice was expelled to form H* that participates in the NIRR, while the water generated H* to timely replenish the hydrogen consumption in titanium hydride lattice.

In the revised manuscript, we have added the Fig. S14 as follows: “

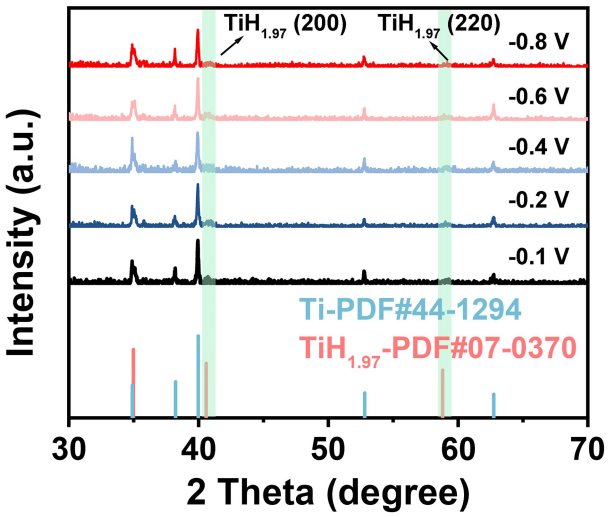

Fig. S14. XRD spectrum of electrode during NIRR at applied potentials of −0.1, −0.2, −0.4, −0.6 and −0.8 V vs. RHE.

(2) In the isotope experiment, we used titanium hydride as the catalyst and using 1 M NaOD + 0.1 M KNO_3 in D_2O solution as the electrolyte for NIRR. After isotopic experiments on titanium hydride catalyst, we characterized the XRD spectrum of the catalyst and found that the (111) crystal plane of the catalyst split into two peaks, while the position of the other peaks did not change.

We have added a detailed description of this conclusion to the revised version:

“After the isotope tracking experiments test, we conducted XRD spectrum on the electrodes. As shown in Fig. S18, compared to $TiH_{1.97}$ before isotope experiments, the (111) crystal plane of the sample exhibited a double peak and a slight shift, which was due to the introduction of deuterium (D). Apart from that, the other diffraction peaks were the same as the characteristic peaks of $TiH_{1.97}$, indicating that the molecular formula of $TiH_{1.97}$ did not change, except that D replaces the H element in the lattice.

This result further verified that lattice hydrogen was involved in the hydrogenation reaction of NIRR, and the hydrogen in water was replenished to lattice hydrogen of $TiH_{1.97}$. This dynamic balance of H* consumption and replenishment improved the efficiency of NIRR."

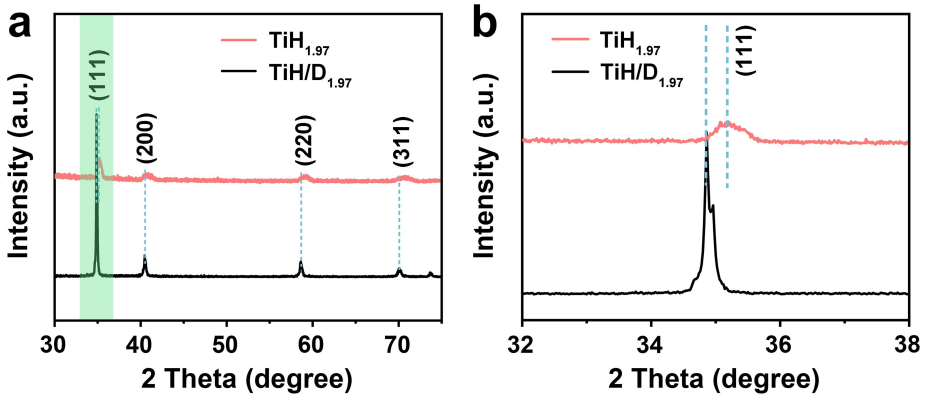

Fig. S18 (a) XRD spectrum of electrode before and after the isotope tracking experiments. **(b)** The local amplification of the characteristic peaks corresponding to the (111) lattice plane.

(3) Similar to the Mars-van Krevelen mechanism reaction, the catalytic mechanism involving lattice nitrogen, lattice chlorine has been reported. These literatures confirmed the dynamic reversible process, and the catalyst did not undergo a phase change during the reaction. As shown in Fig. R10a, *J. Am. Chem. Soc.* ***146****, 14898-14904(2024)* reported the lattice nitrogen of Cu_3N could involve in NIRR reaction, after several tests, they performed detailed characterization of the catalyst and found that the crystal structure, surface composition and size of Cu_3N nanocubes anchored on GDY remained almost unchanged, which indicated that the catalyst had excellent stability. As shown in Fig. R10b, *Angew. Chemie Int. Ed.* ***62****, e202302286*

(2023) had been proved that the XRD of the catalyst did not change before and after the reaction of lattice chlorine, indicating that the phase of lattice chlorine did not change. Through the above analysis, we could see that similar to the Mars-van Krevelen mechanism reaction, the phase of the catalyst would not change. Therefore, in our work, the molecular formula of $TiH_{1.97}$ catalyst did not change before and after NIRR reaction, nor did its phase structure change.

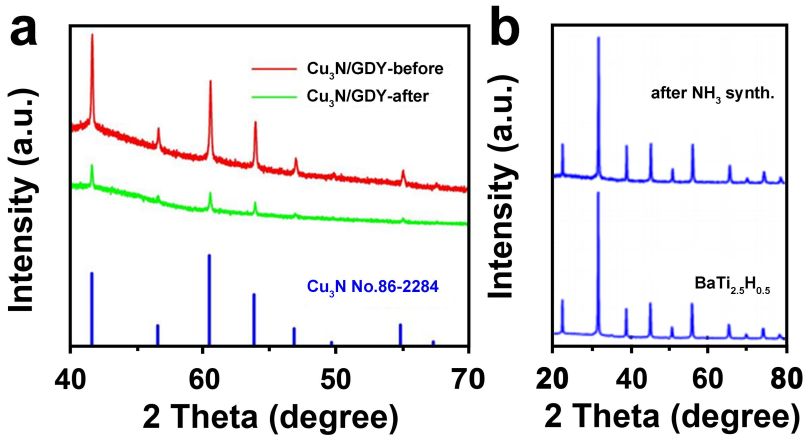

Fig. R10 (a) XRD patterns of Cu_3N/GDY catalyst before and after electrochemical reaction. **(b)** XRD patterns after reaction in 0.5 mol L^{-1} NaCl solution.

5. The FE for ammonia reached the maxima at 50 mM of nitrate (Fig. 3c). Why?

Response: Thank you for your valuable input. We also recognized this issue, so we supplemented the yield and FE around a nitrate concentration of 0.05 M. For nitrate concentrations of 0.02, 0.03, 0.04, 0.05, 0.06, 0.07, 0.08, 0.09, 0.1, 0.2, 0.5 and 1 M, we found that as the nitrate concentration increased, the Faradaic efficiency gradually improved. However, after the nitrate concentration reached a certain level, the FE showed a slight decreasing trend. This phenomenon was presented in the form of a diagram as shown in the Fig. S11 below:

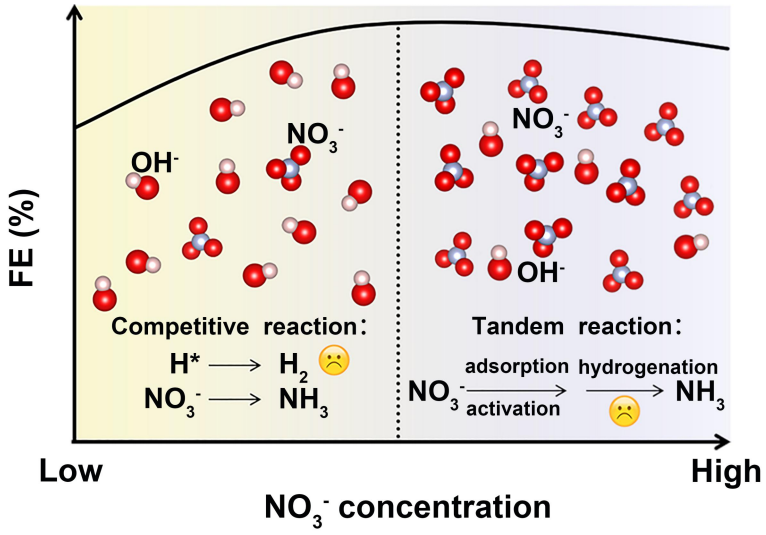

Fig. S11. The schematic diagram of the effect of NO_3^- concentration on FE.

(1) At low nitrate (NO_3^-) concentrations, the competitive reactions between nitrate (NO_3^-) reduction to ammonia (NIRR) and hydrogen evolution reaction (HER) play a dominant role.

In the process of NIRR, NO_3^- first adsorbed on the electrode surface. The adsorbed NO_3^- was then reduced to adsorbed nitrite (NO_2^-) by electrons, which served as one of the rate-determining steps in the electrocatalytic reduction of nitrate. This reaction was accompanied by competing reactions such as hydrogen evolution reaction (HER). Therefore, the initial NO_3^- concentration had a significant impact on the reduction rate. Therefore, increasing the NO_3^- concentration could improve the nitrate reduction activity, inhibit the hydrogen evolution reaction, and thus improve the faradaic efficiency of the NIRR. As shown in the Fig. S10, as the nitrate concentration increased from 0.02 M to 0.06 M, the faradaic efficiency gradually increased from 73.3% to 99.21%.

(2) At high nitrate (NO_3^-) concentrations, the tandem catalytic reaction between nitrate activation and hydrogenation played a dominant role.

For high concentration of NO_3^-, the decisive factor for the efficiency of nitrate reduction reaction was the number of effective active sites on the catalyst surface. The nitrate reduction reaction involved the **adsorption of nitrate** and **the subsequent hydrogenation process**, and the accumulation of a large amount of NO_3^- reduction products hinder the further hydrogenation of the active sites, which would have a certain impact on the FE, leading to a slight decrease in FE. Therefore, continued increase in nitrate concentration would hinder the hydrogenation reaction, slightly reducing the activity of NIRR. As shown in the Fig.S10, further increasing the nitrate concentration from 0.07 M to 1 M showed a slightly decreasing trend in Faradaic efficiency from 99.18% to 93.34%.

(3) In addition to our observation of the rule of FE changing with NO_3^- concentration that FE gradually increased with the increase of NO_3^- concentration at low concentration. When the NO_3^- concentration reached a fixed value, FE slightly decreased with the increase of NO_3^-concentration. A similar phenomenon was also observed in *ACS Catal. (2023) 13, 1513−1521 and Nat. Commun. (2022) 13,1129-1142*, as shown in Fig. R11 and we gave a detailed explanation here.

[Figure redacted]

Fig. R11 (a) Faradic efficiency and ammonia production of Rh NFs for NIRR in the 0.1 M Na_2SO_4 electrolyte (pH 11.5) containing 5, 10, 100, 200, 1000, and 2000 mM NO_3^-, respectively. *(ACS Catal. 2023, 13, 1513−1521)*.(b) The FE of NO_2^- and NH_3, the NH_3 yield rate (Y_{NH3}), as well as the ratio of the formed NH_3 concentration [NH_3] to the converted NO_3^- concentration [NO_3^-] on the CuCoSP catalyst at −0.175 V vs. RHE at [NO_3^-] in the range of 1−100 mM at pH 13.*(Nat. Commun. (2022) 13:1129)*

In the revised manuscript, we have added the corresponding description as follows:

"In addition, as the nitrate concentration increased from 0.02 M to 0.06 M, the FE gradually increased from 73.3 % to 99.2 %. When the concentration continued to increase from 0.07 M to 1 M, FE showed a slight downward trend from 99.2 % to 93.3 %. At low NO_3^- concentrations, the competitive reactions between NIRR and hydrogen evolution reaction (HER) played a dominant role. At high NO_3^- concentrations, the tandem catalytic reaction between nitrate activation and hydrogenation played a dominant role. Their relationship diagram was shown in Fig. S10."

In the revised Supporting Information, we added Fig. S10:

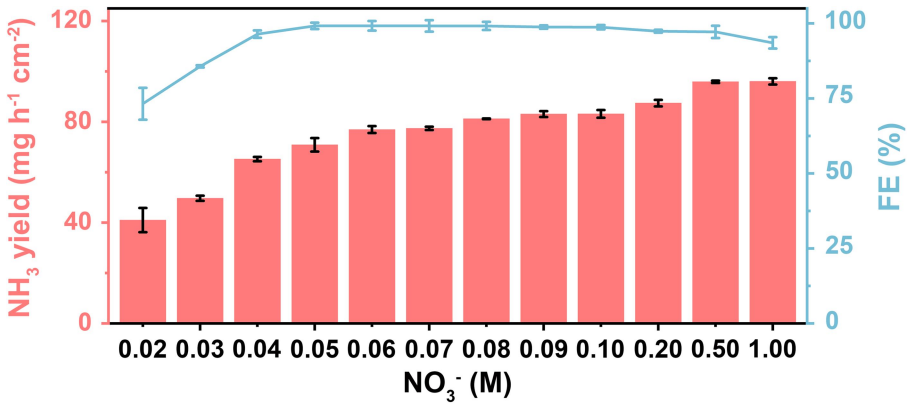

Fig. S10 NH_3 yield and FE for titanium hydride at NO_3^- concentration of 0.02, 0.03, 0.04, 0.05, 0.06, 0.07, 0.08, 0.09, 0.1, 0.2, 0.5 and 1 M.

6.The NIRR performance looks very good compared to all state-of-the-art catalysts according to Fig. 3(f). However, it should be noted that the performance was compared based on "mg/h-cm²". Since the authors used fiber-like electrodes with a high loading of electrocatalyst and a very high ECSA, normalizing by the geometric area of electrode is not fair. The authors should quantify the loading of $TiH_{1.97}$ on the surface and report the activity of their catalyst in mg/h-g or mol/h-g, then compare with other studies to see if this result really outperforms others or not.

Response: We appreciate the valuable comments from the reviewer. To verify that our catalyst has superior catalytic performance compared to other advanced catalysts, we calculated the NH_3 yield and FE of our materials separately by area and weight of titanium hydride, and compared them with other literature reports in a table, with the following specific description:

(1) Compare in unit area (mg h^{-1} cm^{-2}): To verify that our catalyst had superior catalytic performance compared to other advanced catalysts, we had reviewed about

ten papers. Under the same test conditions (1 M KOH + 0.1 M KNO_3), we compared their active surface area (ECSA) and calculated the ammonia production rate per unit active area. Through calculation and comparison, we found that the active surface area of our catalyst was 115.43 cm^2, and the ammonia production rate per unit active area was 0.72 (Table S3). This data indicated that although our catalyst's ECSA was not large, but its NH_3 yield per unit active area surpasses that of other literature. In order to showed the excellence activity of our catalyst more directly, we made a bar chart to compare the NH_3 yield by electrode area, ECSA and ECSA-normalized NH_3 yields (Fig. S15). This result fully demonstrates the excellent catalytic activity of this electrode. Therefore, it was fair to use "mg h^{-1} cm^{-2}" for performance comparison.

(2) Compare in unit mass (mg h^{-1} mg_{cat}^{-1}): Additionally, in order to more fairly verify the superiority of the catalytic activity of titanium hydride in NIRR as the reviewer suggested, we calculated the loading amount of titanium hydride catalyst on the electrode as shown in Fig.S4. To highlight the outstanding performance of this catalyst, we compared it with other literature under the same conditions. As could be seen from Figure S17 and the Table S4, under the same test conditions (1 M KOH + 0.1 M NO_3^-), titanium hydride catalyst still had a significant advantage in terms of NH_3 yield (139.33 mg h^{-1} mg cat^{-1} at −0.7 V vs. RHE) .

In the revised article, we added the corresponding description as follows:

"Under the same conditions (1 M KOH + 0.1 M NO_3^-), the titanium hydride catalyst demonstrated a significantly higher NH_3 yield rate (83.64 mg h^{-1} cm^{-2}) and FE (99.11 %) at the potential of −0.7 V vs. RHE compared to the latest NIRR electrocatalysts documented in the literatures[15, 29, 30, 31, 32, 33, 34, 35, 36, 37], and the ECSA-normalized NH_3 yield up to 0.72, while maintaining NIRR performance that was on par with or superior to that of its competitors (Fig. 3f, Fig. S15, Table S3). In addition, the voltage ranges used in various literatures were different, and we also compared the NIRR performance under the same NO_3^- concentration, our catalyst could achieve high FE and NH_3 yield rate at high voltages as shown in Fig. S16, which was very important in ammonia synthesis, and this performance was difficult to achieve in other catalysts. We also calculated the NIRR performance based on the mass of the titanium hydride catalyst loaded on the electrodes. As could be seen from Figure S17 and the Table S4, under the same test conditions (1 M KOH + 0.1 M NO_3^-), titanium hydride catalyst still had a significant advantage in terms of NH_3 yield (139.33 mg h^{-1} mg cat^{-1} at −0.7 V vs. RHE)."

In the revised Supporting Information, we added the Fig.S4, Fig. S15, Fig. S17 and Table S3, Table S4:

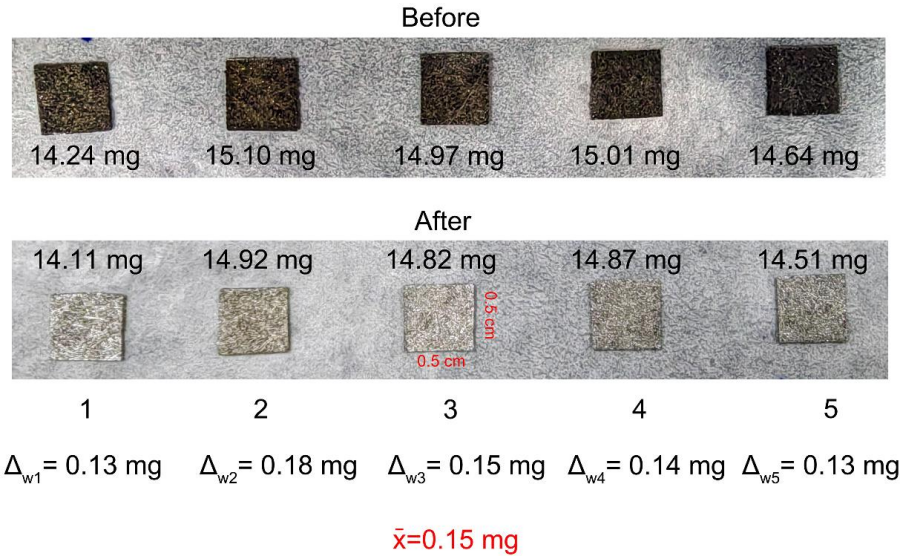

Fig. S4 Weighing the difference in mass before and after the reaction with 0.1 M HCl.

Note: We used the strong oxidizing agent (HCl: 0.1 M) to undergo a chemical reaction with the electrode ($TiH_{1.97}$/Ti). By weighing the difference in mass before and after the reaction (Fig. S4), we could obtain the weight of the titanium hydride loaded on the electrode (data from five sets of measurements were taken and the average was calculated). This was because metal hydrides are highly reactive with hydrochloric acid, while metallic titanium did not react with HCl, so the weight loss on the electrode belongs to titanium hydride. Through calculation, we obtained a titanium hydride loading of 0.6 mg cm^{-2} on the electrodes.

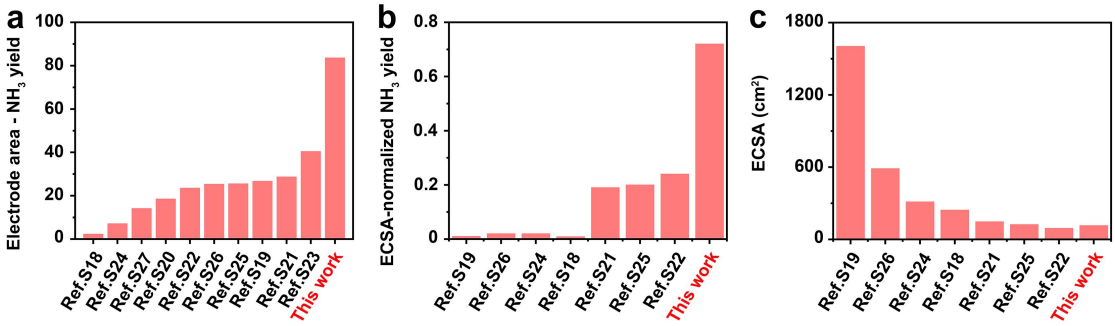

Fig. S15 Comparison of the (a) Electrode area-normalized NH_3 yield (mg h^{-1} cm^{-2}), (b) ECSA-normalized NH_3 yield and (c) ECSA with other literature.

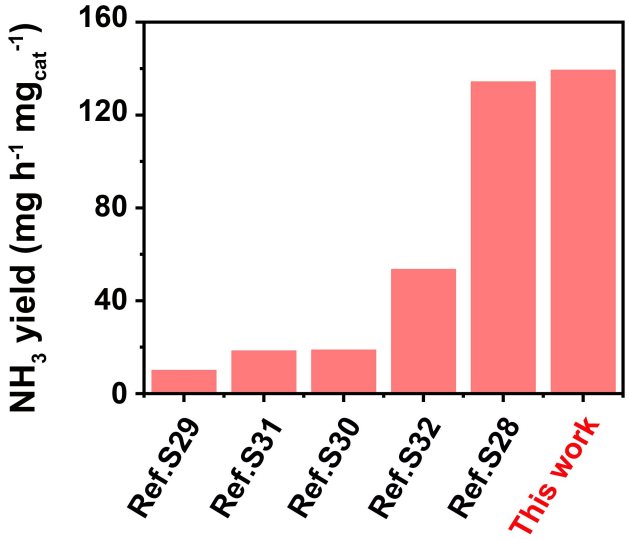

Fig. S17 Comparison of the NH_3 yield with other literature by weight of catalyst powder.

Table S3. The comparison of the NH_3 yield and FE with the reported catalysts for NIRR by the area of electrode and ECSA.

Catalyst	FE (%)	$Yied_{NH3}$ (mg h^{-1} cm^{-2})	ECSA (cm^2)	ECSA-normalized NH_3 yields	Electrolyte	Reduction Potential (vs. RHE)	Reference
$TiH_{1.97}$	99.1	**83.6**	115	**0.72**	1 M KOH + 0.1 M KNO_3	−0.70 V	This work
Cu_x S−$Co_{0.5}$	95.6	**2.3**	243	**0.01**	1 M KOH + 0.1 M KNO_3	−0.40 V	18
o-CoP/C@ Cu_3P/CF	90.3	**26.7**	1603	**0.01**	1 M KOH + 0.1 M KNO_3	−0.25 V	19
$(Cu_{0.6}Co_{0.4})$ $C_{o2}O_4$	96.5	**18.5**	/	/	1 M KOH + 0.1 M NO_3^-	−0.45 V	20
CuO NWAs @Fe_3O_4	97.5	**28.7**	147	**0.19**	1 M KOH + 0.1 M KNO_3	−0.27 V	21
RuO_x/Pd	98.6	**23.5**	92	**0.24**	1 M KOH + 0.1 M KNO_3	−0.50 V	22
CNs@CoP	98.3	**40.4**	/	/	1 M KOH + 0.1 M $NaNO_3$	−0.60 V	23
$Cu_{50}Ni_{50}$	90.0	**7.1**	312	**0.02**	1 M KOH 0.1 M KNO_3	−0.15 V	24
FeB_2	96.8	**25.5**	123	**0.20**	1 M KOH + 0.1 M KNO_3	−0.60 V	25
Cu@C	99.3	**25.3**	587	**0.04**	1 M KOH + 0.1 M KNO_3	−0.70 V	26
CuFe-450	95.1	**14.1**	/	/	1 M KOH + 0.1 M KNO_3	−0.30 V	27

Table S4. The comparison of the NH_3 yield and FE with the reported catalysts for NIRR by the weight of catalyst.

Catalyst	FE (%)	Y_{NH3} (mg h^{-1} mg $_{cat}^{-1}$)	Electrolyte	Reduction Potential (vs. RHE)	Reference
$TiH_{1.97}$	**99.10**	**139.3**	1 M KOH + 0.1 M KNO_3	−0.70V	This work
$AuCu_3$@Au	**86.50**	**134.3**	1 M KOH + 0.5 M NO_3^-	−0.75 V	28
Bi-Cl_{red}	**73.50**	**10.0**	1 M KOH + 0.1 M NO^-	−0.70 V	29
Cu/Cu_xO/GDY	**96.10**	**18.7**	1 M KOH + 0.1 M NO_3^-	−0.70 V	30
Cu_3N/GDY	**84.50**	**18.4**	1 M KOH + 0.1 M KNO_3	−0.70 V	31
2D Fe-cyano	**82.30**	**53.5**	1 M KOH 0.1 M KNO3	−0.60 V	32

7. Fig. S14 has a wrong caption. It should be the data for V.

Response: Thanks to the comments. We have revised the wrong caption in Fig. S26 in this article.

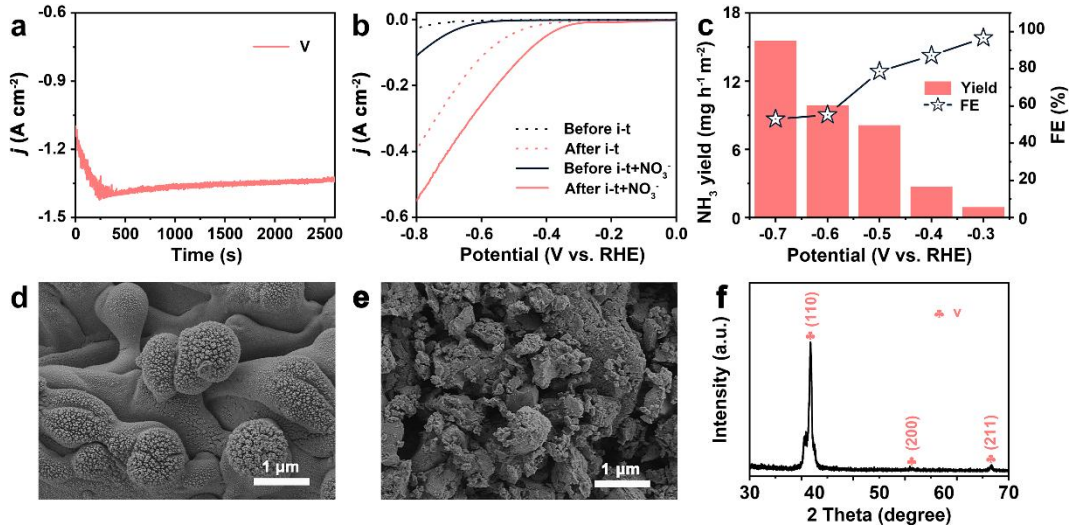

Fig. S26 (a) i-t curves of cathodic electrochemical reconstructed at −1.3 V vs. RHE.

(b) LSV curves. **(c)** NH_3 yields and FEs for V against various work potentials in 1 M KOH solution with 0.1 M NO_3^-. **(d, e)** SEM images of the V before and after cathodic electrochemical reconstructed. **(f)** XRD patterns.

Responses to the review's comments

We have read the referees' comments very carefully and have revised the manuscript thoroughly, considering all the feedback and suggestions. The reviewers' comments and our responses to these comments are listed below. In this response letter, the reviewers' comments are presented in black italics, our responses are in blue, and all changes are marked in red color in the revised manuscript and supporting information. We would like to thank the referees for their helpful comments and expect that we have now produced a more balanced and better account of our work. We trust that the responses and the corresponding revision of the manuscript fulfill the editor's and reviewers' requirements for considering this manuscript for publication in "***Nature Communications***". Nevertheless, if there is any further question about this submission, please feel free to let me know.

Reviewer #4 (Remarks to the Author):

The authors have addressed all comments in a constructive way. The contributions of previous studies and the major contributors of this work compared to previous studies have been emphasized and clarified in the revised manuscript now. With these classifications, the paper can be recommended for the publication in Nature Communications. However, a few minor revisions are required prior to the acceptance of this paper.

1. In addition to the XAFS data, the PXRD data with the comparison to all standard spectra of Ti, TiH_2, and $TiH_{1.97}$ are also very important and informative to show that

the sample here is $TiH_{1.97}$. Thus, I suggest the authors to add Figure R7 in the response to comments into the SI as well with a brief discussion in the main text.

Response: Thank you very much for your professional questions, which are very helpful to improve the quality of our paper.

(1) Inspired by the reviewer's valuable advice, we had added Fig. R7 from the previous review comments to the Supporting Information as Fig. S5, and had included a corresponding discussion in the revised manuscript.

(2) Combining XAFS spectra (Fig. 2d) and XRD spectrum (Fig. S5), it was clear that the characteristic peaks of $TiH_{1.97}$ were distinct from those of TiH_2, therefore, this catalyst had been confirmed as $TiH_{1.97}$.

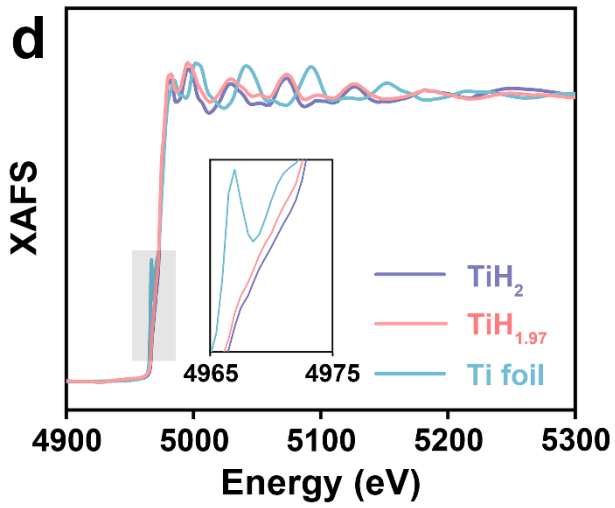

Fig. 2 (d) XAFS spectra at Ti K-edge.

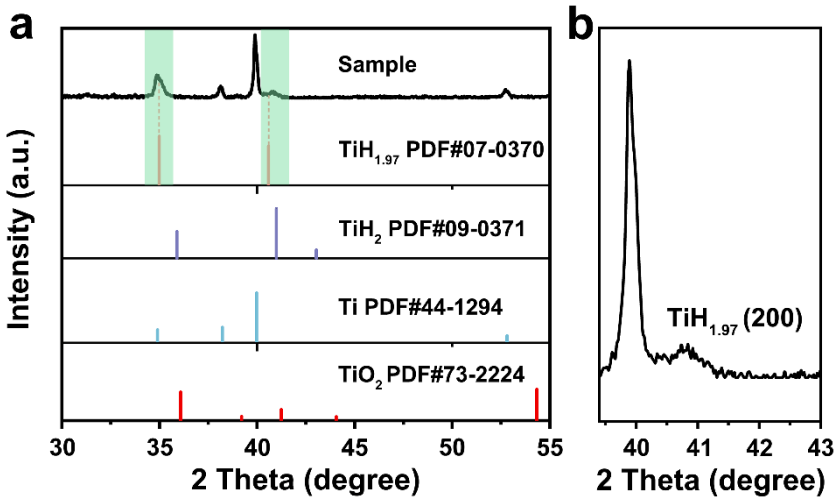

Fig. S5 (a) The XRD spectrum for electrode and the standard spectra of Ti (PDF#44-1294), TiO_2 (PDF#73-2224), TiH_2 (PDF#09-0371) and $TiH_{1.97}$ (PDF#07-0370) and **(b)** the magnified local image of the characteristic peak corresponding to $TiH_{1.97}$ (200).

(3) More importantly, the proposed mechanism of lattice hydrogen participating in catalytic reversible reactions could be extended to other metal hydrides, such as **palladium hydride (Fig. S25), tantalum hydride (Fig. S26), and vanadium hydride (Fig. S27)**.

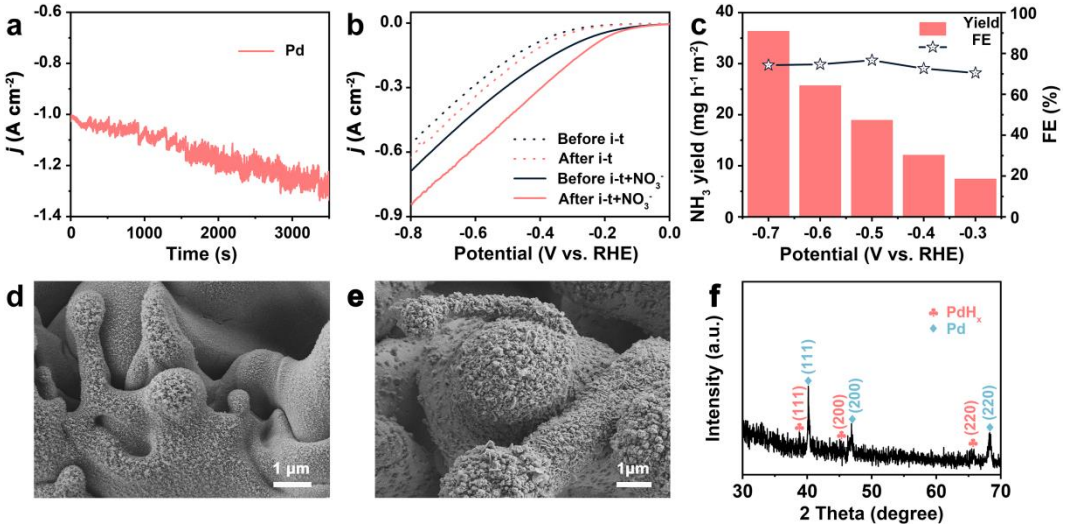

Fig. S25 (a) i-t curves of cathodic electrochemical reconstructed at −1.0 V vs. RHE.

(b) LSV curves. **(c)** NH_3 yield and FE for Pd against various work potentials in 1 M KOH solution with 0.1 M NO_3^-. **(d, e)** SEM images of the Pd before and after cathodic electrochemical reconstructed. **(f)** XRD patterns.

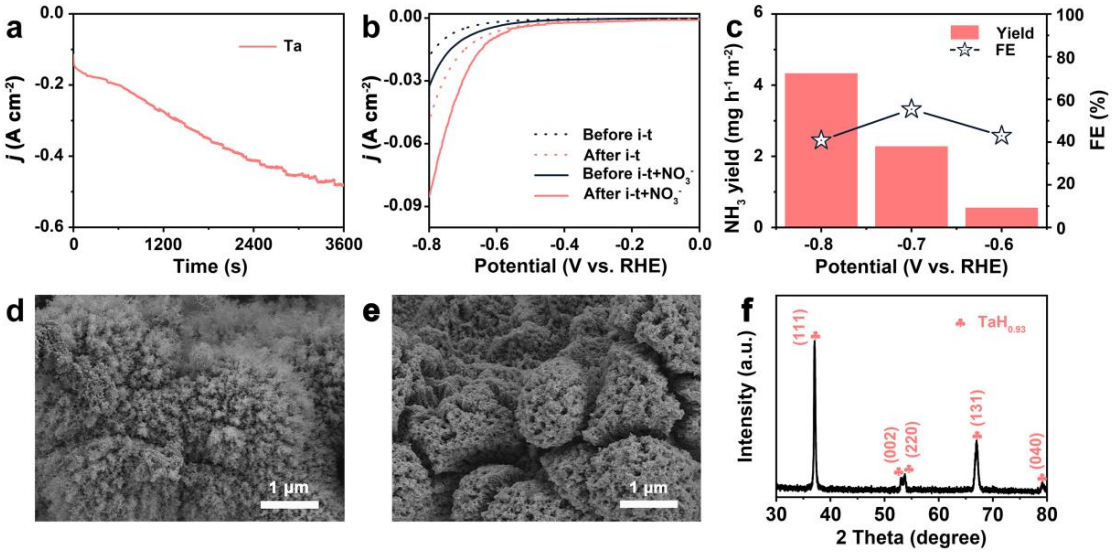

Fig. S26 (a) i-t curves of cathodic electrochemical reconstructed at −0.9 V vs. RHE. **(b)** LSV curves. **(c)** NH_3 yield and FE for Ta against various work potentials in 1 M KOH solution with 0.1 M NO_3^-. **(d, e)** SEM images of the Ta before and after cathodic electrochemical reconstructed. **(f)** XRD patterns.

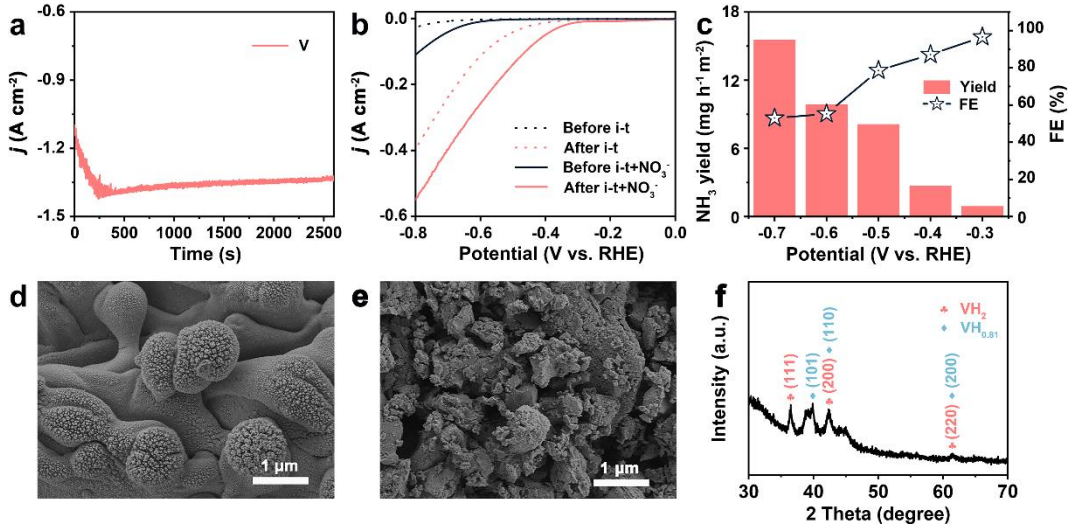

Fig. S27 (a) i-t curves of cathodic electrochemical reconstructed at −1.3 V vs. RHE.

(b) LSV curves. **(c)** NH_3 yield and FE for V against various work potentials in 1 M KOH solution with 0.1 M NO_3^-. **(d, e)** SEM images of the V before and after cathodic electrochemical reconstructed. **(f)** XRD patterns.

In the revised manuscript, we have added the corresponding discussion:

"In addition, we also provided the standard cards for TiO_2 (PDF#73-2224), and TiH_2 (PDF#09-0371) (Fig. S5a), and partially magnified the diffraction peaks at $TiH_{1.97}$ (200) (Fig. S5b). By comparison, we found that there were no characteristic peaks of TiO_2 in the XRD pattern. Combining XAFS spectra (Fig. 2d) and XRD spectrum (Fig. S5), it was clear that the characteristic peaks of $TiH_{1.97}$ were distinct from those of TiH_2, therefore, this catalyst had been confirmed as $TiH_{1.97}$."

In the revised Supporting information, we have added Fig. S5 as follows:

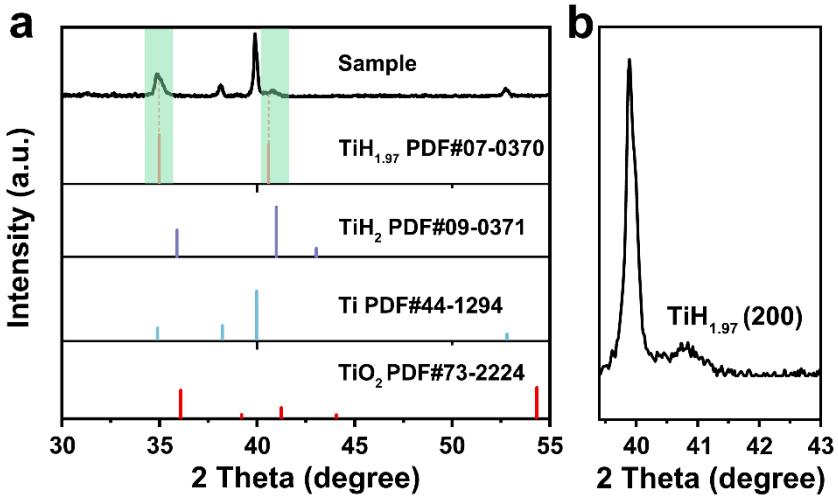

Fig. S5 (a) The XRD spectrum for electrode and the standard spectra of Ti (PDF#44-1294), TiO_2 (PDF#73-2224), TiH_2 (PDF#09-0371) and $TiH_{1.97}$ (PDF#07-0370) and **(b)** the magnified local image of the characteristic peak corresponding to $TiH_{1.97}$ (200).

2. The authors used XRD after electrocatalysis and XRD after isotope experiments to show that the participation of lattice hydrogen in TiH1.97 could be recovered during the NIRR process. But if we look at the XRD data in Figure S14 closely, after the NIRR at some potentials (especially at -0.8 V), the diffraction peaks of TiH1.97 become significantly weaken. Thus, it is most likely that after the reaction at a large overpotential, most lattice hydrogen atoms could not get recovered and the material started to get reduced into titanium. The authors should show the zoom-in data of Figure S14 focusing on these two diffraction peaks, and make some discussions in the revised manuscript.

Response: Thank you for your valuable advice.

(1) In Fig. S14 of NCOMMS-24-31004A, we have flattened the baseline of the XRD curves, which resulted in a visual weakening of the $TiH_{1.97}$ characteristic peak, for which we apologized as this might have caused a misunderstanding for the readers. Therefore, in the revised manuscript, we had modified the ex-situ XRD and added XRD curves after the NIRR at a higher potential (−1.0 V), as well as local magnification of the (200) and (220) characteristic peaks. The modified Fig. S15 showed that the characteristic peak of $TiH_{1.97}$ maintains the original phase even the potential high up to −1.0 V. Thank you again for the reviewer's professional questions, which are very helpful in improving the quality of our manuscript.

(2) As shown in Fig. S1, the current density rose as the applied potential increased, indicating that the higher applied potential led to faster hydrogenation. Therefore, under a large overpotential, the synthesis rate of titanium hydride would be

accelerated, and there would be no phenomenon of titanium hydride being transformed into titanium as mentioned by the reviewer.

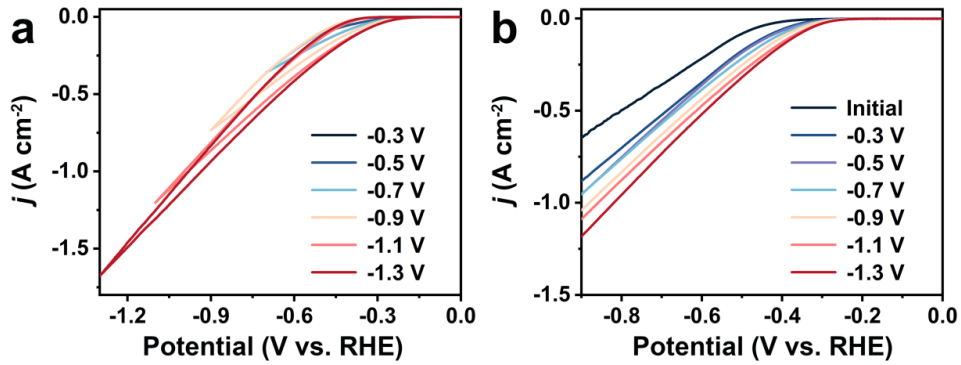

Fig. S1 (a) Cyclic voltammograms within the different range from −0.3 V to −1.3 V vs. RHE. (b) Corresponding polarization curves after (a).

(3) In titanium hydride, the lattice hydrogen spills out and participated in the hydrogenation reaction during the nitrate reduction process, while the H generated by water electrolysis replenishes the hydrogen consumption in titanium hydride. The dynamic equilibrium process of this hydrogen consumption and replenishment was the main point of our article. So, $TiH_{1.97}$ was in a state of dynamic balance between generation and consumption, and would not be converted into titanium even at high potential.

In the revised manuscript, we have added the corresponding description as follows:

"We also tested the XRD spectrum of electrode during NIRR at applied potentials of −0.1, −0.2, −0.4, −0.6, −0.8 and −1.0 V vs. RHE. Based on ex-situ XRD patterns (Fig. S15a) and local magnification of the (200) and (220) characteristic peaks (Fig. S15b, c), the phase of titanium hydride did not change during the NIRR process,

indicating that the Ti to H ratio in the active material remained unchanged. This result also confirmed our proposed viewpoint: In titanium hydride, the lattice hydrogen spills out and participated in the hydrogenation reaction during the nitrate reduction process, while the H generated by water electrolysis replenishes the hydrogen consumption in titanium hydride.

In the revised manuscript, we have added the Fig. S15 as follows: “

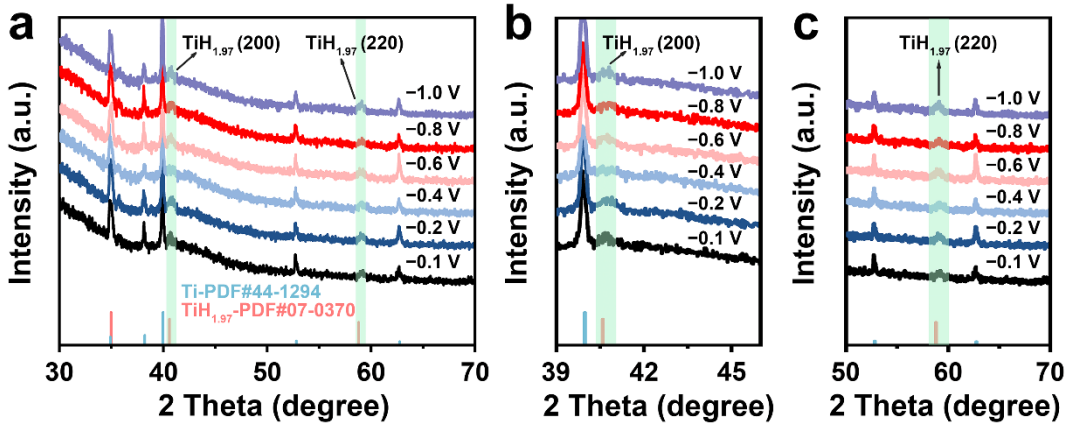

Fig. S15 (a) XRD spectrum of electrode during NIRR at applied potentials of −0.1, −0.2, −0.4, −0.6, −0.8 and −1.0 V vs. RHE. The magnified local image of the characteristic peak corresponding to **(b)** $TiH_{1.97}$ (200) and **(c)** $TiH_{1.97}$ (220).

REVIEWERS' COMMENTS

In this response letter, the reviewers' comments are presented in *black italics*, our responses are in blue.

REVIEWERS' COMMENTS

Reviewer #4 (Remarks to the Author):

Comments have been properly addressed with revisions made in the manuscript and SI, thus the paper can be accepted for publication.

Author reply: We sincerely thank the reviewer for your positive feedback on our work. We are grateful for the valuable comments and suggestions, which have significantly improved our paper to an acceptable standard.